ARE CAFFEINE'S EFFECTS ON NEURONAL CALCIUM LEVELS DUE TO THE CAFFEINE METABOLITE, PARAXANTHINE?

By

Kendra Jean Hartsuyker

A Thesis Presented to

The Faculty of Humboldt State University

In Partial Fulfillment of the Requirements for the

Degree Master of Arts in Psychology: Academic Research

Committee Membership

Dr. Ethan Gahtan, Committee Chair

Dr. Christopher Aberson, Committee Member

Dr. David Baston, Committee Member

Dr. Christopher Aberson, Graduate Coordinator

May 2017

Abstract

ARE CAFFEINE'S EFFECTS ON NEURONAL CALCIUM LEVELS DUE TO THE CAFFEINE METABOLITE, PARAXANTHINE?

Kendra Jean Hartsuyker

Caffeine has diverse effects on neurons including, potentially, protection against Parkinson's-related neurodegeneration. Caffeine may protect neurons from damage by limiting mitochondrial membrane permeability through a calcium-dependent mechanism. This study was a first step investigating calcium's role in caffeine neuroprotection in vivo using zebrafish larvae. Elavl3:GCaMP6s zebrafish, which express a genetically encoded fluorescent calcium indicator protein in most CNS neurons, received caffeine (0, 50, 125, 250 µM, bath applied) in an ascending dose series during fluorescence calcium imaging of a central catecholaminergic nucleus (a proposed zebrafish homolog of the locus coeruleus, a structure affected in Parkinson's disease). Parallel experiments tested effects of an ascending dose series of paraxanthine (0, 40, 100, 200 µM), a neuroactive caffeine metabolite, to assess whether paraxanthine mediates caffeine effects. Five outcomes were measured: spontaneous calcium oscillations, visually-evoked calcium responses, spontaneous swimming activity, visually-evoked swimming, and heart rate (visual responses were evoked by a sudden dimming of ambient illumination). Caffeine and paraxanthine had no effect on the power of low frequency (<2Hz) calcium oscillations, visually-evoked calcium responses, or heart rate, even at the highest doses. High doses of

ARE CAFFEINE'S EFFECTS ON NEURONAL CALCIUM LEVELS DUE TO THE CAFFEINE METABOLITE, PARAXANTHINE?

caffeine and paraxanthine moderately but significantly suppressed swimming speed during visually-evoked behavioral responses. Results suggest that the dose range used was too low to produce expected effects of caffeine. Alternatively, caffeine may affect stressed neurons differently from healthy neurons, a possibility we will examine in similar experiments using MPTP challenge.

Acknowledgments

I would like to thank all the wonderful people in my life who gave their support and encouragement throughout my educational career. Without them, I would not have been able to get to where I am today. I'd like to give homage to my two cats, Shere Khan and Zarzar, who spent countless nights staying up keeping me company me while I worked on this project. I would like to especially thank Dr. Ethan Gahtan for his constant support and mentoring. This thesis and the experience I have gained would not have been possible without Dr. Ethan Gahtan's hard work, effort, and much needed advice.

To my undergraduate students, who without this thesis could not have been completed without their diligent work and hard efforts. Thank you Neha Ahora, Zurain Kajani, Robert O'Callahan, and Michael Wilson.

I would like to further acknowledge my committee members for taking the time to help me through the journey of my educational career. Thank you Dr. Ethan Gahtan, my amazing advisor and committee chair; Dr. Christopher Aberson, a member of my thesis committee and graduate program coordinator; and Dr. David Baston, the final member of my committee.

ARE CAFFEINE'S EFFECTS ON NEURONAL CALCIUM LEVELS DUE TO THE CAFFEINE METABOLITE, PARAXANTHINE?

Table of Contents

List of Tables

List of Figures

ARE CAFFEINE'S EFFECTS ON NEURONAL CALCIUM LEVELS DUE TO THE CAFFEINE METABOLITE, PARAXANTHINE?

List of Appendices

Introduction

Parkinson's disease (PD) is characterized as a neurodegenerative disorder affecting mostly the elderly population. The neurodegeneration targets dopamine (DA) producing neurons in the *pars compacta* of the substantia nigra (SN). The decrease in dopaminergic neurons and subsequent DA loss has been hypothesized as a leading cause to the debilitating degradation of voluntary motor control commonly seen in PD patients. In PD, the root cause of DA cell death is still unknown (Lang & Lozano, 1998). One theory examining mutations in mitochondrial DNA (mtDNA) proposes the propagation of dopaminergic cell death may be due in part to a mitochondrial complex I deficiency in PD patients. The mitochondrial complexes are proteins composing the electron transport chain involved in energy production. Impairment of mitochondrial complex I may lead to a significant increase in a toxic metabolite of DA, called 3, 4-dihydroxy-phenylacetaldehyde (DOPAL), because of a decrease in nicotinamide adenine dinucleotide (NAD), a cofactor for the enzyme responsible for metabolizing DOPAL. (Burke et al., 2004; Lang & Lozano, 1998; Panneton, Kumar, Gan, Burke, & Galvin, 2010; Schapira et al., 1990). With this deficit, DOPAL accumulates in higher concentrations than the average population. DOPAL reacts with H_2O_2 to produce free radicals (Li, Lin, Minteer, & Burke, 2001). The concentrations of free radicals are proposed to occur in high enough concentrations to induce the permeability transition pore (PTP) of the mitochondria to change to its full conductance state (Burke et al., 2004; Kluck, Bossy-Wetzel, Green & Newmeyer, 1997; Li et al., 2001; Scarlett & Murphy,

1997). The PTP is a structure spanning the inner membrane and outer membrane of the mitochondria allowing flow of calcium ions between the matrix and the cytoplasm. Changing the PTP into its full conductance state disrupts the electrochemical gradient causing swelling of the matrix releasing cytochrome *c*, a small protein, into the matrix resulting in apoptotic cell death (Kristal, Matsuda, & Byung, 1996; Li et al., 2001).

Paraxanthine, the primary metabolite of caffeine, has neuroprotective effects on DA cells in models of PD (Guerreiro, Toulorge, Hirsch, Marein, Sokoloff, & Michel, 2008; Xu, Xu, Chen, Schwarzchild, 2010). It is established that the neuroprotective effect of paraxanthine is dependent on activation of ryanodine receptors (Guerreiro et al., 2008). Ryanodine receptors are calcium (Ca^{2+}) release channels located on the outer face of the endoplasmic reticulum (ER) (Fill & Copello, 2002; Verkhratsky, 2005). Mitochondria are physiologically close enough to the ER to create Ca^{2+} "hotspots". These microdomains of Ca^{2+} inhibit the mitochondria PTP from opening in its high conductance state, thus preventing apoptotic cell death (Burke et al., 2004; Li et al., 2001; Mannella, Buttle, Rath, & Marko, 1998; Rizzuto et al., 2003; Rizzuto, DeStefani, Raffello, & Mammucari, 2012; Szalai, Krishnamurth, & Hajnóczky, 1999; Szalai, Csordas, Hantash, Thomas, & Hajnóczky, 2000; Verkhratsky, 2005).

Zebrafish are a widely used model organism in drug discovery. Functional domains within proteins are highly conserved allowing the zebrafish to have a high degree of drug response and physiological similarity to humans. The proposed experiments will take advantage of the ability to measure neuronal calcium dynamics in intact zebrafish larvae using optical methods to investigate how caffeine and

paraxanthine affects intracellular calcium. By establishing the concentrations of both compounds that are effective in activating the release of Ca^{2+} from the ER, these experiments will provide critical information for subsequent studies designed to test whether Ca^{2+} release from the ER protects against PD-related neuronal degeneration. Paraxanthine is an active metabolite of caffeine and has not been tested in the zebrafish before, so a secondary goal of these experiments is to determine to what extent caffeine's effects on neuronal calcium levels depends on the actions of paraxanthine.

Literature Review

Parkinson's Disease

Parkinson's' disease (PD) has been classified as a neurodegenerative movement disorder commonly diagnosed in the elderly population. PD affects approximately 2% of the population over the age of 65 and 4-5% of the population over the age of 85, although these are likely under estimates as under-diagnosis is fairly common (Lang & Lozano; 1998; Eriksen, Dawson, Dickson, & Petrucelli, 2003). Classic PD symptoms have been characterized as bradykinesia, akinesia, rigidity, resting tremors, depression, sleep deficits, and an impaired gait. (Lang & Lozano; 1998). The major symptoms of PD have been linked to a loss of dopaminergic neurons in the Substantia Nigra (SN) and a loss of dopamine (DA) in the Striatum (Burke et al., 2004; Hornykiewicz, 1993; Fearnley & Lees, 1991; Panneton et al., 2010). The nigrostriatal DA neurons are responsible for control over voluntary movements (Grillner & Mercuri, 2002).

Current treatments for PD, including the dopamine precursor drug, L-DOPA, and deep brain stimulation, are focused on increasing DA availability in the synapse or reducing tremors (Benabid, Chabardes, Mitrofanis, & Pollak, 2009; Cesura & Pletscher, 1992; Cools, Barker, Sahakain, & Robbins, 2003; Stefani et al., 2007). These treatments relieve symptoms but do not prevent the continued death of dopaminergic neurons. Therefore, genetic and cellular mechanisms of PD neurodegeneration are under active investigation to identify degenerative processes that may be disrupted to rescue stressed neurons and prevent further cell loss (Luo, Hoffer, Hoffer, & Oi, 2015; McNeill et al., 2013; Winklhofer & Haas, 2011). Some of this research has revealed intracellular

calcium regulation to be a critical process in dopaminergic cell loss and one that could potentially be manipulated therapeutically (Cali, Ottolini & Brini, 2014; Hurley & Dexter, 2012; Mattson, 2012; Orrenius, Nicotera, & Zhivotovsky, 2003; Rizzuto et al., 2003).

Genetic mutations affecting mitochondria in Parkinson's Disease. Many studies have tried to find genes linked to PD predisposition (Klein & Westenberger, 2012; Polymeropoulos et al., 1997). However, these studies are examining nuclear genes and have failed to find correlations, only found small effect sizes, or only accounted for a small percent of PD cases. (Klein & Westenberger, 2012; Polymeropoulos et al., 1997). Examining mitochondrial (mtDNA) may provide insight behind the pathology of PD. mtDNA base pair deletions or insertions have already been identified in the pathology of neurodegenerative diseases such a PD and Alzheimer's disease (Wallace, 1999). Inheritance of mitochondria during cell proliferation varies due to random chance. Understanding the cellular inheritance pattern within an organism is important for understand the role of mtDNA in disease because it explains the phenotypic variance that occurs within cell populations.

Phenotypic expression of symptoms originating from mtDNA mutations are highly variable (Wallace, 1999). If two individuals, even from the same family, have the same mutation in their mtDNA, their phenotypic expression of the mutation may be drastically different. Each cell holds a combination of hundreds mutant and wild type mitochondria and within each mitochondria anywhere between 1,000 and 10,000 copies of mtDNA are contained (Wallace, 1992; Winklhofer & Haass, 2011). Figure 1 shows the

mitochondria in a cell undergoing mitosis. The mutant and wild type mitochondria are randomly divided between the daughter cells. After multiple cellular divisions, genetic variability among the ratio of mutant mitochondria and wild type mitochondria within the cell may develop, and the mutant phenotype may be expressed in cells harboring a greater ratio of the mutant mitochondria. The complex genetic and phenotypic variability among cells with mtDNA mutations within individuals may be a contributing reason the link of mutations in mtDNA and PD has been hard to establish.

Another impairment of normal mitochondrial function associated with PD involves a mutation in mitochondrial complex I, which is the first protein in the electron transport chain, leading to a deficit within PD patients. A deficiency in complex I downregulates the production of nicotinamide adenine dinucleotide (NAD), which is a cofactor needed for the enzyme aldehyde dehydrogenase (ALDH) to break down DOPAL into 3,4-dihydroxyphenylacetic acid (DOPAC) (Burke et al., 2004). A study showed that inhibiting ALDH increases DOPAL concentrations 12-fold when compared to controls (Lamensdorf et al., 2000).

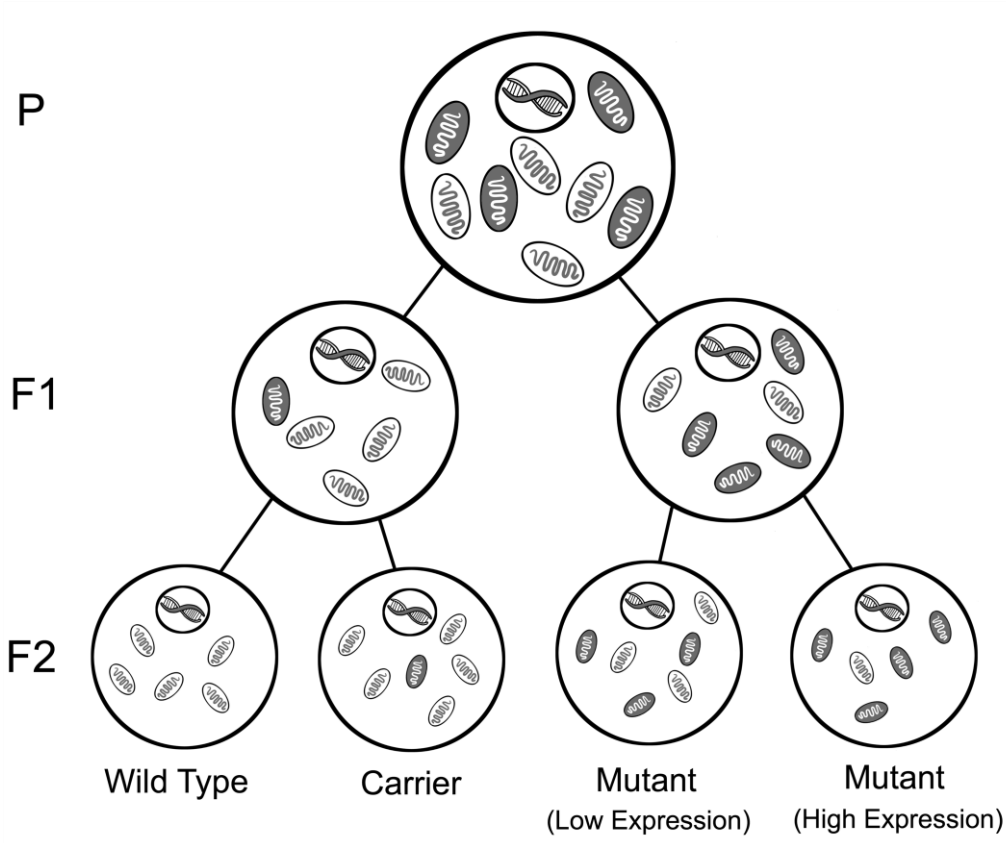

Figure 1. Illustrates how uneven distribution of mutated mtDNA within cells undergoing mitosis can lead to a variety of different phenotypes

Mitochondrial function, dopamine metabolism, and risks for cell death

To understand the impact of a deficiency in complex I of the mitochondria, we must examine the metabolic pathway of DA. Tyrosine is metabolized by tyrosine hydroxylase into L-DOPA. DA is then synthesized from L-DOPA by DOPA decarboxylase in the SN (Burke et al., 2004). Figure 2 shows DA is then metabolized into 3, 4-dihydroxyphenylacetaldehyde (DOPAL) by monoamine oxidase (MAO) (Cesura & Pletscher, 1992). It is important to note hydrogen peroxide (H_2O_2) is also formed in the same reaction during the metabolism of DA into DOPAL (Burke et al., 2004).

In humans, there are two distinct isoforms of MAO: MAO-A, located on the cytosolic face of the mitochondria in the neurons, and MAO-B, located in the surrounding astrocytes (Burke et al., 2004). MAO-A is the only MAO isoform responsible for DA metabolism in striatal DA neurons (Fornai et al., 2000).

Although naturally forming, DOPAL is an unstable molecule, this instability can make DOPAL toxic under certain cellular conditions, such as in the presence of H_2O_2 (Burke et al., 2004; Panneton et al., 2010). Normally DOPAL is rapidly cleaved by aldehyde dehydrogenase (ALDH) into a less volatile molecule, DOPAC (Cesura & Pletscher, 1992; Fornai et al., 2000; Panneton et al., 2010).

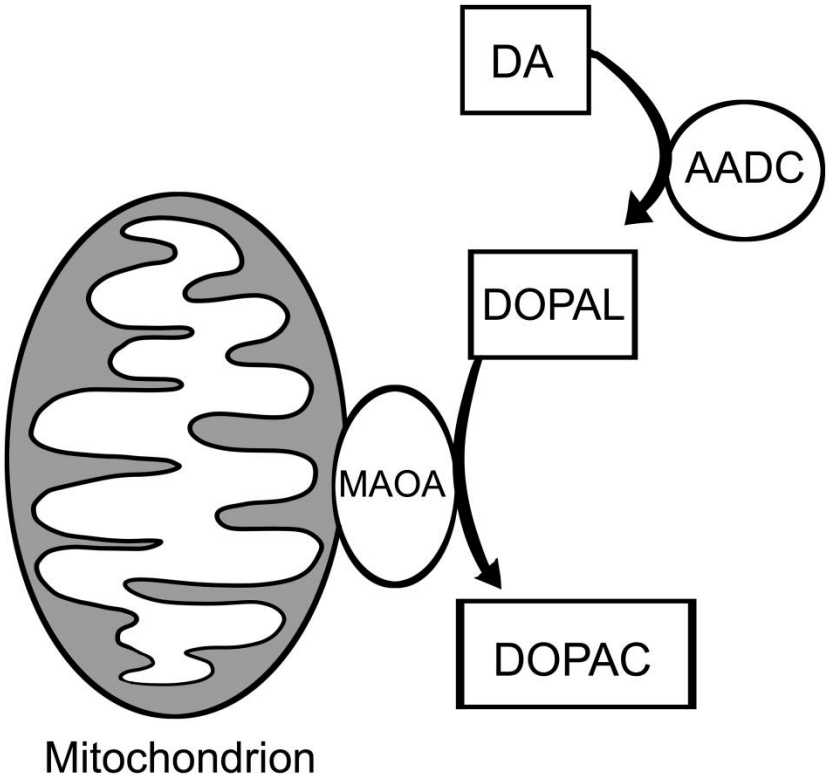

Figure 4. Shows the location of the metabolic pathway of dopamine. The boxes represent compounds and the circles represent enzymes. MAO-A, located on the cytosolic face of the mitochondrion, metabolizes dopamine into DOPAL. The temporal location of DOPAL and H2

Evidence of DOPAL's Toxicity

The most common PD medication, L-DOPA, is a metabolic precursor to DA. By increasing the precursor compound, L-DOPA treatment increases DOPAL concentrations downstream in the dopaminergic pathway. PD patients already experience higher than average DOPAL levels due to a deficiency in mitochondrial complex I. Here we examine how L-DOPA treatment, already causing an increase in DOPAL, may be interacting with a mitochondrial complex I deficiency, a separate mechanism increasing DOPAL, to further propagate dopaminergic cell death.

Evidence shows DOPAL, the primary metabolite of DA, can be toxic under certain circumstances to the cells it is formed in, particularly for dopaminergic cells within the SN (Panneton et al., 2010). The *pars compacta* of the SN, which is the group of neurons controlling reward and movement, was particularly more affected by DOPAL, due to the high concentrations of dopaminergic neurons, than the *pars reticulata* of the SN, which has a relatively high concentration of GABAergic neurons (Panneton et al., 2010). This is suggestive DOPAL is selectively toxic to DA neurons. An analysis of postmortem human brain tissue from healthy donors showed an average DOPAL concentration of 2.3 μM within the SN (Kristal, Conway, Brown, Jain, Ulluci, Li, & Burke, 2001). This concentration was not found to be toxic to the cells. However, an *in vivo* study showed that a slightly higher DOPAL concentration, 6 μM, is toxic to neurons (Kristal et al., 2001). Injections of DOPAL into rat brains resulted in the loss of DA neurons with concentrations of DOPAL as low as 100 ng (Burke et al., 2004). However, injections at concentrations of 500 ng of DA showed no effects on DA neurons (W.

Burke et al., 2004). Although DA is closely related to DOPAL, DA itself is not toxic unless present in large concentrations, approximately 1M (Burke, Li, Williams, & Zham, 2003; Burke et al., 2004; Filloux & Townsend, 1993; Kristal et al., 2001).

L-DOPA, the most common PD medication, significantly increases DOPAL concentrations. Injections of 10 µM of DA through dialysis probes into rat brains increased DOPAL by 2,790% ±62 when compared with baselines (Fornai et al., 2000). Similarly, injections of 50 mg/kg of L-DOPA through dialysis probes into rat brains increased DOPAL levels by 1,861% ±70when compared to controls (Fornai et al., 2000). In both experiments, DOPAC, the metabolite of DOPAL, did not experience a significant increase. This is indicative of a "build up" of DOPAL within the brain. L-DOPA treatments may lead to concentrations of DOPAL reaching toxic levels within cells.

In PD patients, the aforementioned mitochondrial complex I deficiency combine with L-DOPA treatment may cause a significant increase in the cellular concentration of the toxic compound DOPAL, furthering the propagation of DA cell death. The mechanism of DOPAL mediated toxicity has been attributed to the production of free radicals in the presence of H_2O_2 (Burke et al., 2004; Li et al., 2001). As mentioned above, H_2O_2 is produced in the same reaction DOPAL is metabolized from DA (Burke et al., 2004). The authors note the mechanism the free radicals are formed is unknown and a recent literary search shows it is still unknown (Li et al. 2001). Free radicals are able to induce the mitochondrial PTP into its full conductance state causing mitochondrial swelling and the release of apoptotic proteins (Kristal et al., 1996; Li et al., 2001). This

points to a therapeutic target by preventing free radicals from inducing the mitochondrial PTP into its full conductance state.

The mitochondria's major role within the cell is regulation of energy metabolism and regulation of apoptotic pathways. Figure 3a shows the structure of mitochondria. It is important to understand mitochondria structure for energy production and regulation of apoptosis. Figure 2a shows mitochondria have two membranes, the outer membrane that segregates the mitochondria from the intracellular environment (cytoplasm) and the inner membrane that segregates the center of the mitochondria (matrix) from the intermembrane space. These properties allow the generation of proton gradient across membranes within mitochondria, and the dissipation of those proton gradient to drive the production of adenosine triphosphate (ATP).

The mitochondrial PTP plays a critical role in normal mitochondrial function by regulating the conductance of calcium between the matrix and the cytoplasm (Azarashvili, Stricker, & Reiser, 2010; Ichas & Mazat, 1998; Patergnani et al., 2011; Rizzuto et al., 2012; Szalai et al., 2000). Changes in the PTP activity can also contribute to apoptosis (Azarashvili et al., 2010; Ichas & Mazat, 1998; Klucket al., 1997; Szalai, Krishnamurthy, & Hajnoczky 1999).

Figure 3b shows the mitochondrial PTP is comprised of three proteins spanning the outer membrane of the mitochondria to the matrix (Arrazola, Silva-Alvarez, & Inestrosa, 2015; Azarashvili et al., 2010). One protein, the voltage dependent anion channel (VDAC) is located on the outer membrane. A second component, adenine nucleotide translocase (ANT) spans the inner membrane. The third component,

cyclophilin D (CypD) is located on the matrix side of the inner membrane and is released during PTP mediated cell death (Arrazola et al., 2015; Azarashvili et al., 2010).

The mitochondrial PTP operates in two distinct pathways, one controls Ca^{2+} signaling and the other controls the effector phase of apoptosis (Ichas & Mazat, 1998). The PTP controls these pathways by openning in two different conductance states (Ichas & Mazat, 1998). Figure 3b shows the conformation changes the VDAC, ANT, and CypD proteins undergo to alter the conductance states and change the flow of Ca^{2+} ions (Arrazola et al., 2015). The low conductance state is a regular part of maintaining cellular Ca^{2+} homeostasis and normal cell functioning (Ichas & Mazat, 1998).

The high conductance state stabilizes the channel in a permanent open conformation resulting in apoptosis (Ichas & Mazat, 1998). This causes an irreversible dissipation of the membrane potential resulting in the loss of mitochondrial structure through swelling of the mitochondrial matrix (Ichas & Mazat, 1998). The swelling forces the outer mitochondrial membrane to burst resulting in the release of the apoptotic proteins into the cytoplasm (Burke et al., 2004; Ichas & Mazat, 1998; Kothakota et al., 1997; Kluck et al., 1997; Orrenius et al., 2003; Scarlett & Murphy, 1997; Youle & Strasser, 2008).

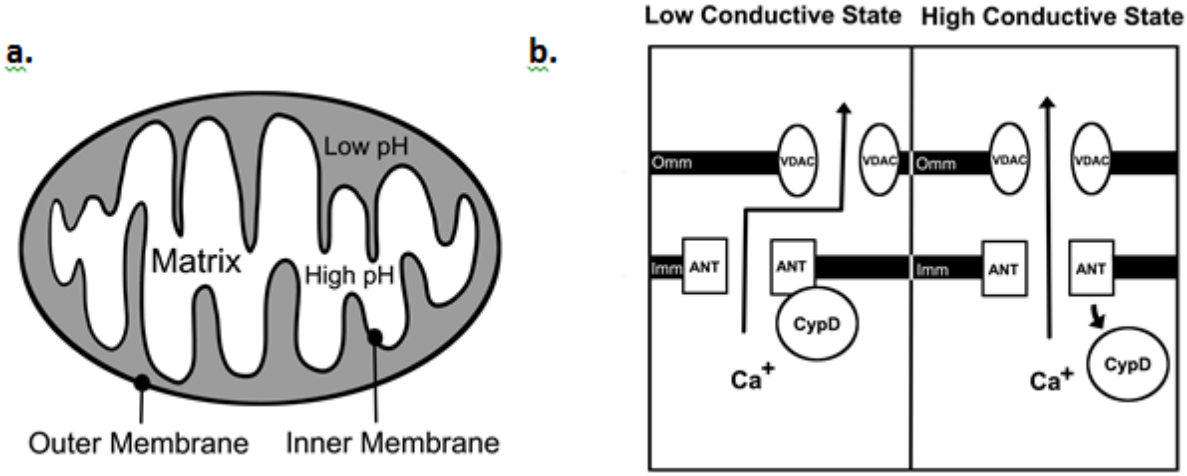

Figure 7. **a.** The structure of the mitochondrion illustrating the low pH of the intramembrane space and the high pH of the matrix. **b.** Represents the mitochondrial permeability transition pore. The low conductance state shows a low flow of calcium ions exiting the matrix to the cytoplasm. The high conductance state illustrates a high flow of calcium ions exiting the matrix, along with the release of the protein CypD

Figure 8. Quantification of spontaneous calcium fluorescence. A. Raw confocal video stack consisting of 6,000 frames. B. Projection of average pixel values across the stack. Arrow heads show individual neuron cell bodies the tart nucleus that can be resolved. C. Threholded image showing isolation of the target nucleus as a density (particle) of blue pixels. A smaller particle in the upper right of the image is not included because of a size cut off. D. Isolated region of interest for subsequently measuring each from in the stack. E. an example plot, from the same trials as panels A-D, showing calcium fluorescence dynamics cross 20 minutesFigure 9. **a.** The structure of the mitochondrion illustrating the low pH of the intramembrane space and the high pH of the matrix. **b.** Represents the mitochondrial permeability transition pore. The low conductance state shows a low flow of calcium ions exiting the matrix to the cytoplasm. The high conductance state illustrates a high flow of calcium ions exiting the matrix, along with the release of the protein CypD

Interaction of DOPAL with the Mitochondrial PTP. During the metabolic breakdown of DA into DOPAL by MAO-A, H_2O_2 is formed as well. DOPAL interacts with H_2O_2 forming free radicals (Burke et al., 2004). MAO-A is active on the cytosolic face of the mitochondrial membrane less than 50 nm away from the mitochondrial PTP (Burke et al., 2004). Concentrations of DOPAL as low as 125 nM create enough free radicals to induce the high conductance state of the mitochondrial PTP, resulting in apoptosis (Burke et al., 2004). The temporal location of free radicals formation relative to the PTP allows for the free radicals to easily interact with the pore. This points to a potential therapeutic target for PD namely, preventing the mitochondrial PTP from entering its high conductance state by forcing the PTP to stabilize into its low conductance state.

Paraxanthine as a Neuroprotectant

Approximately 80% of caffeine gets metabolized into paraxanthine in the liver (Benowitz, Jacob, Mayan, & Denaro, 1995). It is important to note caffeine does not get metabolized during its first pass through the liver (Arnaud, 1993). Caffeine is both hydrophilic and lipophilic (Bonati, Latini, Galletti, Young, Tognoni, & Garattini, 1982). Caffeine and paraxanthine share many pharmacological properties and actions, including lipophilic properties (Denaro, Brown, Wilson, Jacob, & Benowitz, 1990). These properties allow caffeine and paraxanthine to freely pass through all biological membranes and the blood-brain barrier through simple diffusion and saturable carrier-mediated transport (Arnaud, 2011; McCall, Millington, & Wurtman, 1982; Verkhratsky,

2002). Approximately 80% of caffeine passes into the brain during its first circulatory pass (Oldendorf, 1971).

Studies have shown that the consumption of caffeine is negatively correlated with risk for PD (Ascherio et al., 2001; Kalda, Yu, Oztas, & Chen, 2006; Xu et al., 2010). This link has been supported by experimental studies, showing caffeine and its metabolites have neuroprotective effects against PD-related toxicity such as that caused by exposure to the selective DA neuron toxin, MPTP (Xu et al., 2002; Xu et al., 2010).

The neurotoxin MPTP is the metabolic precursor to the biologically active molecule MPP+. MPTP is the gold standard for modeling PD as it induces similar pathologies similar to those seen in PD in humans. Once MPP+ reaches DA neurons, it interferes with mitochondrial complex I of the electron transport chain inducing permanent Parkinsonian symptoms (Smeyne & Jackson-Lewis, 2005).

Originally, the neuroprotective effects of caffeine and paraxanthine were thought to result from inhibition of adenosine receptors (Ascherio et al., 2001; Checkoway et al., 2002; Chen et al., 2001; Kalda et al., 2006). However, research suggests the neuroprotective effects are directly related to the opening of ryanodine receptors, Ca^{2+} release channels, and the subsequent rise in intracellular Ca^{2+} concentration (Guerreiro et al., 2008). Ryanodine receptors are Ca^{2+} release channels located on the ER (Fill & Copello, 2002; Verkhratsky, 2006).

Guerreiro et al. (2008) modeled PD through MPP+ exposure in differentiated midbrain DA cells in a culture. Examining the dose-dependent neuroprotective effects of caffeine and paraxanthine, they showed equal concentrations of paraxanthine had a

significantly larger neuroprotective effect than caffeine. This is suggestive that the neuroprotective effect of caffeine is, in part or in full, due to its metabolite paraxanthine. The neuroprotective effect is caused by ryanodine receptor activation, rather than adenosine receptor blockade. Activation of ryanodine receptors, using the agonist dantrolene, exhibited similar neuroprotective effects when compared to paraxanthine. Whereas blockade of ryanodine receptors, using a ryanodine receptor antagonist, prevented the neuroprotective effects. Paraxanthine mediated activation of ryanodine receptor results in a moderate elevation of intracellular cytosolic free calcium (Ca_{cyt}^{2+}) levels. A large increase in Ca_{cyt}^{2+} did not have a neuroprotective effect, suggesting the Ca_{cyt}^{2+} concentration needs to be elevated just above normal levels to have a neuroprotective effect.

Paraxanthine is most neuroprotective being treated for 10 days continuously after MPP+ exposure at concentrations between 800 - 1000 μM treated in differentiated brain cells. The researchers identified neuroprotection by quantifying cells expressing tyrosine hydroxylase, the enzyme responsible for synthsizing L-DOPA. The paraxanthine treatment group showed 194% more TH cells in the culture over the control group. Critically, the degree of intracellular Ca^{2+} increases was correlated with the number of preserved dopaminergic neurons. The preserved dopaminergic neurons also retained basic functioning such as the synthesis, release, and uptake of DA.

While these experiments provided compelling evidence of the mechanism of neuroprotection by caffeine, it must be emphasized that in this *in vitro* study the neurons were exposed to much higher paraxanthine concentrations that would be expected after

ingestion of caffeine in living animals (Burke et al., 2004). The authors note it would be expected to see similar effects in vivo when exposed to lower concentrations (Guerreiro et al., 2008).

Role of Intracellular Calcium in the Neuroprotective Effects of Caffeine

Calcium overview. Calcium is an important signaling molecule used in many aspects of cell regulation. The fluctuation of Ca^{2+} regulates cell excitability, synaptic plasticity, neurotransmitter release, gene regulation, and apoptosis (Fill & Copello, 2002; Mattson, 2012; McConkey & Orrenius, 1997; R. Rizzuto et al., 2012; Usachev, Shmigol, Pronchuk, & Verkhratsky, 1993). Ca^{2+} is widely recognized as the most important signaling molecule and is highly regulated in neurons (Mattson, 2012).

Elevations of intracellular Ca^{2+} levels are necessary for cell signaling, however prolonged increases in Ca^{2+} can result in cell death (Hongpaisan, Winters, & Andrews, 2004; Ichas & Mazat, 1998; McConkey & Orrenius, 1997; Orrenius et al., 2003; Rizzuto et al., 2003). Ca^{2+} signaling requires cells to signal using brief elevations of Ca^{2+} levels followed by a rapid decay, commonly known as Ca^{2+} oscillations (Berridge, Lipp, & Bootman, 2000; Dupont, Abou-Lovergne, & Combettes, 2008). There are three types of Ca^{2+} encoding are amplitude modification (AM), frequency modification (FM), and amplitude and frequency modification (AFM) (De Pitta, Volman, Levine, & Ben-Jacob, 2009). With AM encoding, the strength of the stimulus is encoded by changes in amplitude while frequency remains constant. FM encoding encodes the strength of the stimulus in varying frequencies while the amplitude remains the same. AFM encoding is a combination of AM and FM encoding, where the strength of the stimulus is encoded in

a blend of changes in both frequency and amplitude. They type of encoding a cell uses varies based on the type of cell.

Cells are suspended in a high Ca^{2+} concentration (in the mM range) extracellular environment (Fill & Copello, 2002; McConkey & Orrenius, 1997). Resting free Ca^{2+} concentration within the cytoplasm is much lower (approximately 100 nM range) than the extracellular environment (Berridge et al., 2000; Fill & Copello, 2002; McConkey & Orrenius, 1997). The cytoplasm is filled with Ca^{2+} buffering and binding proteins to prevent large influxes of Ca^{2+} inducing apoptosis (Fill & Copello, 2002; Verkhratsky, 2005).

Calcium in the Endoplasmic Reticulum. The ER is the largest intracellular organelle present in all nerve cells and is recognized as the most prominent storage facility for Ca^{2+} ions (Rizzuto et al., 2012, Verkhratsky, 2005). Neurons use changes in Ca^{2+} levels as an intracellular signal in many cellular functions such as second messengers by activating protein kinases, trigger synaptic vesicle exocytosis, and trigger apoptosis (Brose, Petrenko, Sudhof, & Jahn, 1992; Hongpaisanet al., 2004; McConkey & Orrenius, 1997; Orrenius et al., 2003; Rizzuto et al., 2003; Rizzuto et al., 2012). In neurons, the ER extends throughout dendrites, axons, and soma (Verkhratsky, 2006). Changes in local concentrations of intracellular Ca^{2+} are able to induce signals that diffuse throughout the cell and elicit cellular processes at a remote location (Rizzuto et al., 2012).

There are two main types of Ca^{2+} release channels on the ER: Ryanodine receptors and Inositol trisphosphate receptors (Verkhratsky, 2006). Ryanodine receptors

are large transmembrane proteins located on the outer face of both the smooth and rough ER (Blaustein & Golovina, 2001; Fill & Copello, 2002). Ryanodine receptor channels are large conductance Ca^{2+} channels that are able to move large numbers of Ca^{2+} ions (Fill & Copello, 2002). This large efflux of Ca^{2+} from the ER allows for highly concentrated Ca^{2+} 'hotspots' to form between the ER and mitochondria. Ryanodine receptors control Ca^{2+} flow in a bell-shaped dose-dependent fashion meaning activation of the receptors reliably release Ca^{2+} in a bell shaped curve (Bezprozvanny, Waltras, & Ehrlich, 1991; Fill & Copello, 2002; Verkhratsky, 2005). Ryanodine receptors are inactive when exposed to nM and mM concentrations of ryanodine receptor agonists, but active while exposed to μM concentrations (Bezprozvanny et al., 1991). This feature of ryanodine receptors allows the testing of varying concentrations of paraxanthine to find the ideal concentration for neuroprotection.

Inositol trisphosphate receptors and ryanodine receptors each have a unique way of releasing Ca^{2+} as a cellular signal. Inositol trisphosphate receptors cause Ca^{2+} to release in small 'puffs'. These 'puffs' produce diverse amplitudes resulting from a varying number of channels opening within a cluster (Berridge et al., 2000). This suggests activation of inositol trisphosphate receptors affect AM encoded Ca^{2+} signaling. Ryanodine receptors cause Ca^{2+} to release in 'sparks'. These 'sparks' occur when a cluster of ryanodine receptors open in unison causing a spontaneous spike of Ca^{2+} to be released (Berridge et al., 2000, Cheng, Lederer, & Cannell, 1993). This suggests activation of ryanodine receptors affect FM encoded Ca^{2+} signaling.

Approximately 80% of ryanodine receptors are found facing the cytoplasm, suggesting a release of Ca^{2+} from the ER into the cytoplasm (Verkhratsky, 2002). Free Ca^{2+} ions cannot travel further than 500 nm before being bound by calreticulin, the main Ca^{2+} binding protein in neurons, rendering the Ca^{2+} unable to make cellular changes. (Verkhratsky, 2002). This allows for isolated Ca^{2+} microdomains within the cytoplasm before becoming inactivated through a Ca^{2+} binding proteins.

A study showed 80% of mitochondria were found to be in contact with the ER (Cascarano, Montisano, Pickett, & James, 1982; Copeland & Dalton, 1959). Using GFP labeling of organelles, a study identified the mitochondria and ER were found to be localized at less than 200 nm apart (Rizzuto et al., 1998). This localization was labelled the mitochondria associated membrane (MAM) (Rizzuto et al., 1998). The ER and MAM play a pivotal role in Ca^{2+} exchange into the mitochondria through ryanodine receptors and inositol trisphosphate receptors. The MAM allows for Ca^{2+} 'hotspots' to form so signaling between the ER and mitochondria occurs without interruption of Ca^{2+} binding proteins. This allows for adequate functioning of mitochondrial metabolism and is a determinant in cell life and death (Cascarano et al., 1982; Ichas & Mazat, 1998; Kluck et al., 1997; Patergnani et al., 2011; Raturi & Simmen, 2013).

Mitochondria sense these localized 'hotspots' of Ca^{2+} and rapidly uptake the Ca^{2+}. The mitochondria react to the Ca^{2+} 'hotspot' as normal cellular Ca^{2+} signaling (Ichas & Mazat, 1998). The fast rate of Ca^{2+} uptake triggers the mitochondrial PTP to open under a low conductance state. (Ichas & Mazat, 1998). Administering caffeine and paraxanthine will cause Ca^{2+} 'hotspots' to form within the MAM. This treatment will artificially force

the PTP into stabilizing into its low conductance state preventing PTP mediated apoptosis. Manipulating the mitochondria PTP may be a new therapeutic target to treat PD patients in the future.

Zebrafish as a Model Organism in PD Research

General. The zebrafish, *Danio rerio*, have emerged as a leading model organism for drug discovery and toxicology research. The zebrafish is small in size and easy to house in large numbers. They provide simple detection of target phenotypes making them essential for high-throughput screening (Zon & Peterson, 2005). Using a whole organism allows researchers to answer biological questions that cannot be addressed *in vitro* (Zon & Peterson, 2005). The zebrafish provide a high degree of genetic and physiological similarity to mammals. The zebrafish's forebrain dopaminergic nucleus is a homolog of mammalian midbrain dopaminergic system (Lam, Korzh, & Strahle, 2005). As well as, amino acid sequence conservation of proteins between mammals and the zebrafish suggest similar protein functions (Ahmad, Noldus, Tegelenbosch, & Richardson, 2012). This is indicative of a high conservation in drug response between and humans, estimated around 95% (Zon & Peterson, 2005).

Zebrafish embryos and larvae have transparent skin. This feature makes it possible to detect functional and morphological changes in internal organs without killing or dissecting the organism. Transparent skin allows the use of Ca^{2+} imaging with fluorescent dye to quantify changes in Ca^{2+} concentration within the neurons of intact zebrafish larvae.

Caffeine, in non-chronic dosing, affects locomotor behaviors in a dose-dependent fashion (Holtzman, 1989). Examining the swimming speeds in caffeine treated (10, 25, 50 mg/L) zebrafish, showed that at 25 mg/L and 50 mg/L concentration caused a decrease in swimming speed (Ladu et al., 2015). It is important to note our experiment will be using much lower concentrations of caffeine. However, there is no change in swimming behaviors in concentrations less than 100 μM (Abdelkader, Chang, Kim, Song, Kim, & Park, 2013; Capiotti et al., 2011).

Zebrafish larvae have an average baseline heart rate of approximately 130 bpm (*SD = 6.3)* (Burns, Milan, Grande, Rottbauer, MacRae, & Fisherman, 2005). Caffeine concentrations of 100 μM, exposed to zebrafish embryos, significantly increased heart rate (Abdelkader et al., 2013). This study measured heart rate immediately after administration and at 48, 72, and 96 hours post fertilization (hpf). The average heart rate in the control group was 110, 110, and 112 bpm at 48, 72, and 96 hpf respectively. The average heart rate in the 100 μM group was 122 at 72 hpf and 136 at 96 hpf. It is important to note this study was conducted in zebrafish embryos. The planned experiment will be using zebrafish larvae so heart rate is expected to be higher than the embryos.

Statement of the Problem

Evidence shows that paraxanthine exhibits neuroprotective effects *in vitro* (Guerreiro et al., 2008; Xu et al., 2002; Xu et al., 2004). This study was designed as another step toward developing information needed to evaluate the potential for clinical applications of paraxanthine neuroprotection, by examining parathanxine effects on neurons in an in vivo vertebrate model system. Specifically, I examined effects of paraxanthine and caffeine in living zebrafish larvae to determine whether these drugs have equivalent, dose-dependent effects on neuronal calcium dynamics, locomotor activity, and heart rate. I did not directly assess neuroprotective effects of caffeine or paraxanthine. Instead, this study was intended to obtained baseline dose-response information on these drugs to inform future neuroprotection studies.

Hypotheses

Hypothesis 1. Bath application of paraxanthine and caffeine will increase the amplitude of calcium oscillations from forebrain dopamine neurons in 5 dpf zebrafish in a dose-dependent manner.

Hypothesis 1a. Amplitude of calcium oscillations during successive 20-minute imaging blocks will significantly increase as paraxanthine concentration in the bath solution is increased from 0 to 40 µM to 100µM to 200 µM.

Hypothesis 1b. Amplitude of calcium oscillations during successive 20-minute imaging blocks will significantly increase as caffeine concentration in the bath solution is increased from 0 to 50 µM to 125 µM to 250 µM.

Hypothesis 1c. Similar amplitudes will be found for the effects of paraxanthine and caffeine on intracellular calcium oscillations.

Rationale for Hypothesis 1. Paraxanthine is an agonist for ryanodine receptors, ER calcium release channels. Paraxanthine is a main metabolite of caffeine, so I reasoned that a comparable amount of either drug should both produce similar changes in calcium oscillations. The forebrain dopamine nucleus that was imaged is a putative homolog of a mammalian catecholamine nucleus, the locus coeruleus, that is affected in PD (Lam et al., 2005).

Hypothesis 2. Bath application of paraxanthine and caffeine will increase visually-evoked (light-dimming-evoked) intracellular calcium responses in forebrain dopamine neurons in 5 dpf zebrafish in a dose-dependent manner. These hypotheses paralleled Hypotheses 1a-1d but examined neuronal calcium increases evoked by a visual stimulus rather than examining resting calcium levels. These hypotheses were tested in the same group of animals by presenting the sensory stimulus twice at the end of each 20-minute imaging block using to measure resting calcium.

Hypothesis 2a. The size of visually-evoked calcium responses (measured as the percentage change in fluorescence intensity from before to immediately after the stimulus) will significantly increase as paraxanthine concentration in the bath solution is increased from 0 to 40 µM, to 100µM to 200 µM.

Hypothesis 2b. The size of visually-evoked calcium responses will significantly increase as caffeine concentration in the bath solution is increased from 0 to 50 µM to 125 µM to 250 µM.

Hypothesis 2c. A similar dose-response function (slope) will be found for the effects of paraxanthine and caffeine on the size of visually-evoked calcium responses.

Rationale for Hypothesis 2. Paraxanthine is an agonist for ryanodine receptors, ER calcium release channels. Paraxanthine is a main metabolite of caffeine, so the comparable amount of should both produce similar increases in calcium. Previous studies determined that light dimming reliably evoked action potentials within these neurons in untreated zebrafish larvae. Calcium is increased inside neurons for up to 1s when an action potential is fired (Grienberger & Konnerth, 2012). An increase in fluorescence immediately following the visual stimulus was therefore considered as a stimulus-evoked neuronal response.

Hypothesis 3. Bath application of paraxanthine and caffeine will increase resting heart rate in 5 dpf zebrafish larvae.

Hypothesis 3a. Bath application of 200 µM Paraxanthine for 20 minutes will increase heart rate 5 minutes later.

Hypothesis 3b. Bath application of 250 µM Caffeine for 20 minutes in 5 dpf zebrafish larvae will increase heart rate 5 minutes later.

Hypothesis 3c. Bath application of Paraxanthine or Caffeine for 20 minutes in 5 dpf zebrafish larvae will have a similar affect heart rate.

Rationale for Hypothesis 3. Caffeine administration increases heart rate in the zebrafish (Abdelkader et al., 2013). Paraxanthine is the main metabolite of caffeine. By using a metabolically equivalent ratio of paraxanthine to caffeine, I reasoned that the larvae should show the same behavioral effects. Heart rate was measured in this

experiment as a manipulation check because if the drug application procedure worked as expected a change in heart rate should occur.

Hypothesis 4. Bath application of paraxanthine and caffeine will decrease spontaneous swimming activity (measured as the percentage of time spent in motion during a 20-minute observation period) in 5 dpf zebrafish larvae in a dose-dependent manner.

Hypothesis 4a. Swimming activity will significantly decrease as paraxanthine concentration in the bath solution is increased from 0 to 40 µM to 100 µM to 200 µM.

Hypothesis 4b. Swimming activity will significantly decrease as caffeine concentration in the bath solution is increased from 0 to 50 µM to 125µM to 250 µM.

Hypothesis 4c. Changes in spontaneous swimming activity will remain similar between the caffeine and paraxanthine treated zebrafish.

Rationale for Hypothesis 4. Acute caffeine dosage decreases active voluntary behaviors, such as spontaneous swimming behaviors, in a dose dependent manner (Holtzman, 1989; Ladu et al., 2015). Paraxanthine is the main metabolite of caffeine. By using a metabolically equivalent ratio of paraxanthine to caffeine I reasoned that the larvae should show the same behavioral effects. This thesis focused on cellular mechanisms of caffeine and paraxanthine but it is important to measure behavioral effects of these drugs because much of PD research with zebrafish uses swimming behaviors as a secondary measure of dopaminergic cell death, and future paraxanthine neuroprotection studies would be expected to use both neuronal and behavioral measures of function.

Method

Subjects

Zebrafish are housed and bred on the HSU campus in BSS 122 F. Animals care and breeding procedures are described in detail in a facility manual (standard operating procedures) that has been filed with the Humboldt State University IACUC for this zebrafish facility. For the current study approximately 10 adult zebrafish from the existing colony (approximately 5 male and 5 female) will be used as brood stock to generate larvae for experimentation. Approximately 105 larvae, ages 4-8 days post fertilization, will be used in experiments.

At 5 days post fertilization (dpf), larvae will be randomly assigned to one of three conditions, consisting of 8 larvae each. Prior research on calcium response in zebrafish neurons (n = 27) found a minimum of a 10% change in fluorescence within 24 cells when compared to baseline measurements (Gahtan, Sankrithi, Campos, &O'Malley, 2002).

Table 1

Experimental Design and Dosages

	Caffeine	Paraxanthine
Control	N/A	N/A
Caffeine – Low	50 µM	N/A
Caffeine – Med	125 µM	N/A
Caffeine - High	250 µM	N/A
Paraxanthine – Low	N/A	40 µM
Paraxanthine – Med	N/A	100 µM
Paraxanthine – High	N/A	200 µM

Note. The study design is a 2x3 mixed factorial experiment with repeated measures.

Table 1 shows the first factor is drug type, with two levels, caffeine and paraxanthine, compared between subjects. The second factor is drug concentration, with three levels (a low, intermediate, and high concentration of each drug) compared within subjects. There are four dependent measures: the first measure, resting neuronal calcium fluorescence, measured as the percent of pre-drug fluorescence intensity, the second measure, sensory-evoked neuronal calcium responses using a dark-flash stimulus and measured in neurons known to be activated during dark-flash responses, the third measure, spontaneous swimming activity, and the fourth measure, sensory-evoked swimming activity using a dark-flash stimulus. The same animals were used to measure both spontaneous and evoked calcium levels (measures one and two) and calcium fluorescence was measured repeatedly in the same animals. A different group of animals were used for behavioral measures (the same group for spontaneous and evoked swimming activity), and measurements of swimming behavior were also made repeatedly within animals across drug concentrations.

Multiple neurons within the target nucleus can be recorded simultaneously in a single animal and I had originally proposed analyzing each imaged neuron as a separate observation (I performed a statistical power analysis to determine that each group should include at least 8 neurons measured across at least 4 animals, to achieve statistical power of at least .80, assuming a large effect size). However, resolving individual neurons proved to be unreliable in the recorded images, so instead each nucleus was analyzed as a single observation. In preparations where both sides of the brain could be resolved clearly in the same image, I recorded two nuclei per animal, but in most preparations only one

nucleus was recorded. In total, 25 nuclei were imaged across 15 larvae and 14 of those nuclei were included in the final statistical analysis.

Instruments and Software

Data from zebrafish behavior will be captured using two cameras. The high speed PTEM Photon Focus camera and the time lapse Pixelink camera. These will be used to obtain behavioral data from stimuli sent by a LabJack controlled program with DAQFactory. The images obtained will be analyzed by a custom script to be run through ImageJ. Images of dopaminergic cells and calcium signaling will be taken with an Olympus Fluoview FV1000 confocal microscope using the appropriate lens.

Procedures

Calcium imaging. I proposed using one of two methods for fluorescent calcium imaging in zebrafish neurons, either by first injecting a calcium-sensitive fluorescent dye into neurons, or by using a transgenic zebrafish line with a genetically-encoded fluorescent calcium indicator (GECI) protein expressed in neurons. The GECI line was the preferred option and I was able to obtain a suitable zebrafish line, called elavl3:GCaMP6s (doi:10.1038/nmeth.3040), from the lab of Florian Engert at Harvard (after securing required permissions from both universities). This line expresses a GECI in most brain neurons under the control of the elavl3 gene, which is a transcription factor expressed in newly differentiated neurons. Therefore, no injections were done, and all calcium imaging was performed in 5 days post fertilization (dpf) GCaMP6s larvae that were confirmed to have inflated swim bladders (a sign of general health).

Larvae are prepared for calcium imaging by first being embedded in low-melting temperature agarose (ThermoFisher; 1.2% dissolved in egg water). Larvae are place with a transfer pipette onto a clean plastic surface in a small drop of egg water and then re-aspirated into a new pipette containing about 1ml of the melted agar solution (at about 28 deg C). Once suspended in the agar the larva is dripped onto a microscope cover slide, where within 20 seconds it will be immobilized (usually in the desired dorsal-up posture) within the hardening agar. The cover slip is then inserted into a custom imaging chamber that allows the agar holding the larva to be in contact with a fluid solution that can be changed rapidly and remotely, thus allowing different drug solutions to be introduced during the imaging session without moving the larva (once in contact with the porous agar, drug solutions diffuse through the agar, contact the larva's skin, and are taken up through the skin to the larva's blood circulation. The imaging chamber is then clamped onto the heated stage plate (maintained at 23 deg C) of the confocal microscope. An Olympus FV1000 confocal system with a 20x .95NA water immersion objective will be used for imaging calcium indicator fluorescence. First, a cell of interest will be identified and documented in a saved anatomical reference image. The cells of interest include any of the glutamatergic descending neurons in the hindbrain (Kinkhabwala et al., 2011). The image will be optically magnified so the cell occupies the central portion of the imaging area. To assess baseline fluorescence the confocal will be set to automatically acquire an image of the cell once every 10 seconds for 10 minutes (an imaging block). The normal egg water in the imaging chamber will then be removed and replaced with egg water containing 50 μM caffeine, and another 10 min imaging block will be run. Two

more imaging blocks will follow, changing the caffeine solutions between each, first to 125 µM and finally to 250 µM. These concentrations of caffeine were determined from previous research that examined zebrafish larvae responses to caffeine (Abdelkader et al., 2013). Four imaging blocks will also be run in paraxanthine experiments, with the solution changed between blocks as follows: 0, 40 µM, 100 µM, and 200 µM. Administration of paraxanthine in the zebrafish have yet to be documented. Paraxanthine concentrations were determined by using proportions based on caffeine metabolic pathway concentrations. After imaging the larva will be de-embedded from the agar (done with fine tools under a dissecting microscope) and returned to an individual 35mm petri dish containing approximately 3ml of regular egg water. Approximately 24 hours after the calcium imaging experiment larvae will be assessed for mortality so that potential toxicity from the previous drug exposures might be detected, and following this assessment all larvae still living will be euthanized by immersion in 0.03% tricaine methanesulfonate for 10-20 minutes following cessation of opercular movement.

Table 2

Timeline for Calcium Imaging Experiments

Condition	Data Acquired	Time for Procedure	Cumulative Time
Control (pre-drug)	Heart rate imaging	2min	2 min
	Spontaneous Ca^{2+} imaging	20 min	22 min
	Dark flash Ca^{2+} imaging trials	4 min	26 min
50μM Caffeine or	Heart rate imaging	2min	28 min
40μM Paraxanthine	Spontaneous Ca^{2+} imaging	20 min	48 min
	Dark flash Ca^{2+} imaging trials	4 min	52 min
125μM Caffeine or	Heart rate imaging	2min	54 min
100μM Paraxanthine	Spontaneous Ca^{2+} imaging	20 min	74 min
	Dark flash Ca^{2+} imaging trials	4 min	78 min
250uM Caffeine or	Heart rate imaging	2min	80 min
200uM Paraxanthine	Spontaneous Ca^{2+} imaging	20 min	100 min
	Dark flash Ca^{2+} imaging trials	4 min	104 min

Note. Each larva received all concentrations within caffeine and paraxanthine groups. All control, caffeine, and paraxanthine solutions also contained 100μM d-tubocurarine to prevent movement during imaging. Solutions were changed manually between imaging blocks using a plastic pipette. Agar-embedded larvae were bathed in approximately 2ml of each solution during image. N = 15 nuclei in eight larvae for the caffeine group, and N = 11 nuclei in six larvae for the paraxanthine group.

Spontaneous Locomotor Behavioral Swimming Test. Larvae, at 6 dpf, will be individually transferred, via plastic pipette, into 10mm wells containing 4 mL of egg water positioned above a digital camera. The camera will be programmed to take images at 1 Hz for 10 minutes each hour for a duration of six hours. The camera utilizes an infrared light source, otherwise the experiments will be conducted in darkness to avoid any vision mediated influences on locomotor behaviors. Post recording, larvae will be pipetted back into a 60mm petri dish and housed in the incubator.

Behavior Analysis. At 6 dpf, larvae will be moved to singular 10 mm wells holding 4 mL of egg water for imaging of behavioral activity. Spontaneous locomotor time lapse recordings will be taken over the course of 6 hours for each group to be used as a baseline. Using a custom script to quantify activity, the stacked images will be subtracted from each other. This will leave us a new video only showing pixels that have changed over the course of the 6 hours, thus providing us with just the fish's swimming behavior. A custom script will then provide an analysis of the fish's locomotor activity in each well providing us with percent of time the fish was in motion during the recording period.

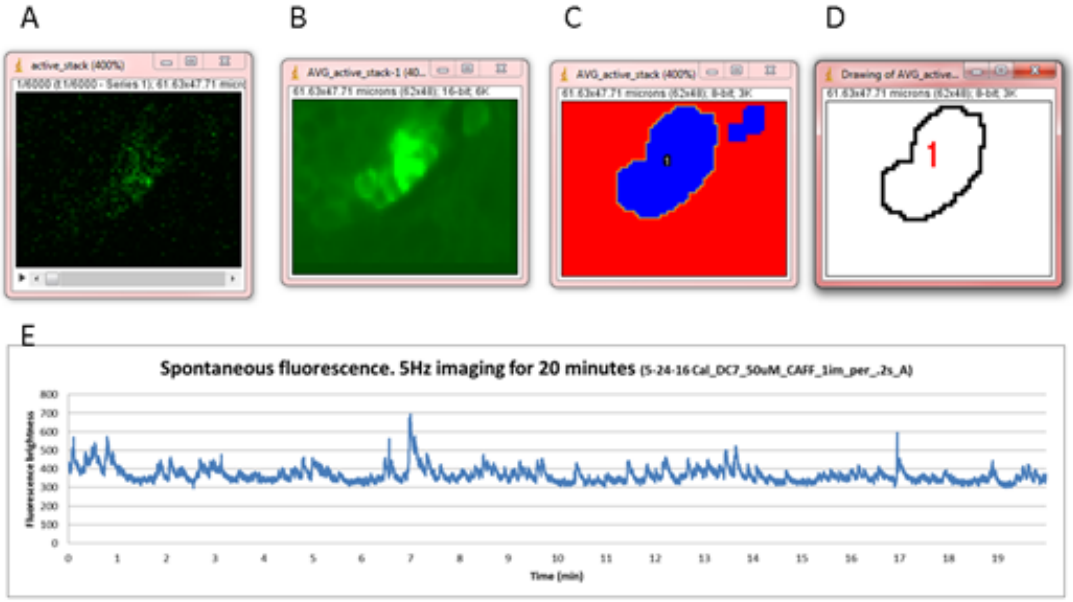

Figure 10. Quantification of spontaneous calcium fluorescence. A. Raw confocal video stack consisting of 6,000 frames. B. Projection of average pixel values across the stack. Arrow heads show individual neuron cell bodies the tart nucleus that can be resolved. C. Threholded image showing isolation of the target nucleus as a density (particle) of blue pixels. A smaller particle in the upper right of the image is not included because of a size cut off. D. Isolated region of interest for subsequently measuring each from in the stack. E. an example plot, from the same trials as panels A-D, showing calcium fluorescence dynamics cross 20 minutes

Figure 11. Example of a visually-evoked calcium imaging trial. A-D. Confocal time lapse projection showing average fluorescence intensity during 4 seconds at the start of the trial scan (A), immediately before the dark flash stimulus (B), immediately after the stimulus (C), and at the end of the scan (D). E. The corresponding fluorescence intensity plot. Colored boxed indicate the time periods shown in A-D. Calculations of ΔF from fluorescence intensity before and after stimulus onset is shown.*Figure 12.* Quantification of spontaneous calcium fluorescence. A. Raw confocal video stack consisting of 6,000 frames. B. Projection of average pixel values across the stack. Arrow heads show individual neuron cell bodies the tart nucleus that can be resolved. C. Threholded image showing isolation of the target nucleus as a density (particle) of blue pixels. A smaller particle in the upper right of the image is not included because of a size cut off. D. Isolated region of interest for subsequently measuring each from in the stack. E. an example plot, from the same trials as panels A-D, showing calcium fluorescence dynamics cross 20 minutes

Heart Rate. Larvae will be embedded in a low melting point agar on a microscope slide. The larvae will not be anesthetized, as we will be analyzing the treatment's effects on heart rate. This require unimpaired functioning of the nervous system. The larvae will be placed under a microscope to record heart rate 1 minutes. A stage warmer is unnecessary as the larvae will spend a total time under the microscope of approximately 5 minutes. The larvae will be removed from the agar and placed into a 60mm petri dish with standard egg water. The petri dish will be housed in an incubator (temperature of 28.5° C; 12h/12h light/dark cycle).

Analyses

Spontaneous calcium dynamics. To draw a region of interest (ROI) around the target nucleus for analysis, each 20 minute video, consisting of 6,000 frames (5 images per second for 20 minutes), was first merged into a single averaged frame (averaged value of each pixel across images). The averaged frame was then thresholded into a binary image that isolated the nucleus as a group of pixels. That pixel group was saved as a ROI file and then applied to each frame of the video to measure fluorescence brightness within that region (Figure 4).

I had originally intended to analyze drug effects on fluorescence brightness as a secondary indicator of intracellular calcium levels. However, because successive 20min imaging blocks were separated by blocks of heart rate imaging, the viewing field had to be moved (from the brain to the heart) and microscope settings changed, and upon returning to the brain nucleus I could not be sure that absolute fluorescence brightness was directly comparable to the previous imaging block. Therefore, I analyzed drug

effects on fluorescence dynamics within imaging blocks, rather than on brightness. Specifically, I examined the power (amplitude) of fluorescence oscillations at specific frequencies within each 20 min imaging block. Spontaneous, low frequency (<5Hz) calcium oscillations are common in neural circuits across species and can be altered by drugs and neurological disease states (Kastanenka et al., 2017), therefore, it is a relevant indicator of caffeine and paraxanthine effects on neurons in the current study. The imaging parameters used in this study (5 Hz for 20 minutes) limited analysis to oscillation frequencies ranging from 0.001 to 2.5 Hz. A spectral analysis of brightness values was performed in Matlab to determine the mean power spectral density (amplitude) in each of the following 5 frequency analysis bins (bins were determined a priori based on constraints of the data and previous research; (Ashworth & Bolsover, 2002; Romano, Peitri, Perrez-Schuster, Jouary, Haudrechy, & Sumbre, 2015, Smeyne & Jackson-Lewis, 2005): 0.001 – 0.01 Hz, 0.01 – 0.05 Hz, 0.05 – 0.1 Hz, 0.1 – 1 Hz, 1-2.5 Hz.

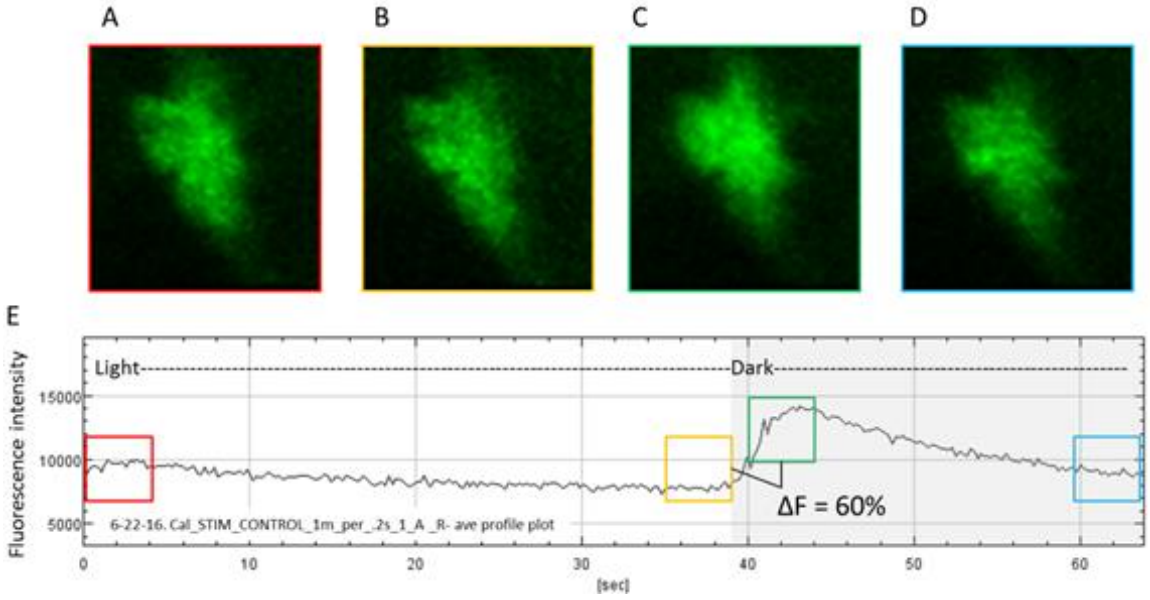

Figure 13. Example of a visually-evoked calcium imaging trial. A-D. Confocal time lapse projection showing average fluorescence intensity during 4 seconds at the start of the trial scan (A), immediately before the dark flash stimulus (B), immediately after the stimulus (C), and at the end of the scan (D). E. The corresponding fluorescence intensity plot. Colored boxed indicate the time periods shown in A-D. Calculations of ΔF from fluorescence intensity before and after stimulus onset is shown.

Visually-evoked calcium responses. ROIs around the target neurons were generated as described for spontaneous fluorescence analysis. Each startle trial lasted 60 seconds with the dark flash stimulus occurring after 30 seconds. A normalized index for stimulus induced fluorescence change (ΔF) was created by dividing the average fluorescence during the four second preceding the stimulus from the average fluorescence during the 4 seconds following the stimulus. This ΔF index, corresponding to the percentage increase in fluorescence, was the dependent measure analyzed for drug and drug concentrations effects on startle trials. Figure 5 shows and example of a visually-evoked calcium response from the present study.

Heart rate. Heart motility was visible in the videos as a pixel contrast oscillations within a limited region of the image. An analysis window was manually drawn around this pixel region using ImageJ and the average brightness within the region was measured on each frame. Brightness values were imported into Microsoft Excel and a formula was applied that detected frames that were brighter than both adjacent frames (the adjacent frames being those captured 200ms before and 200ms after the target frame), indicating a repeated phase of the cardiac rhythm. The number of those repeated phases during the 1 minute recording was divided by 60 to calculate average beats per second.

Swimming behavior. For each drug and dose combination a 1,260 frame behavior video was generated that contained 20 minutes of spontaneous swimming (1,200 frames) followed by a dark flash startle trial (60 frames). A background subtraction method was first applied by subtracting an image that was the averaged pixel values across the entire video, from each video frame, creating a new video where each

frame highlighted the pixels that identified each larva's current position. The video was then thresholded to set non-target pixels to zero, a procedure that is required for automated detection of the XY coordinates of target pixels. An analysis region was drawn around dish and the particle analysis function in *ImageJ was* used to record XY coordinates for each larva on each video frame. The distance formula (distance = sqrt (x2 - x1)^2 + (y2 - y1)^2) was used in Excel to convert successive XY coordinate pairs into the distance traveled by the larvae from frame to frame in units of millimeters per second (this was straight forward as the recoding rate was 1 frame per second). From this, the measure that was analyzed was total distance traveled across 20 minutes. For startle trials a response index was created by dividing the distance traveled during the 60 seconds before the startle stimulus from the distance traveled during the following 60 seconds of darkness. Figure 6 shows steps of the analysis procedure for an example behavior video.

.

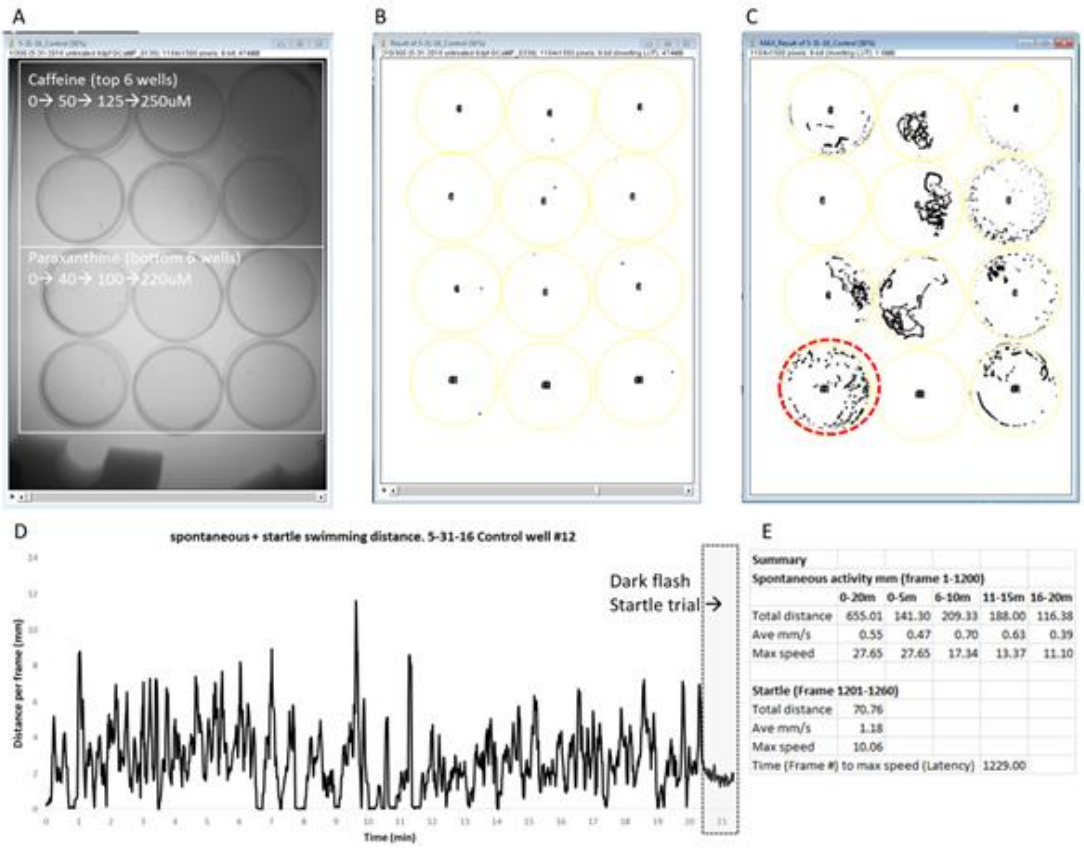

Figure 16. Example of behavioral analysis procedures for a single 20 minute spontaneous activity trial followed by a 1 minute startle trial (taken from a control condition recording). A. Raw image stack of larvae in behavior recording wells. Caffeine and Paraxanthine larvae from the same clutch were tested at the same time to avoid confounds. B. Images have been processed by background subtraction and thresholding and circular regions of interest manually drawn around each well (ROI numbers appear at the center of each well and the larvae can also be seen inside most of the wells as a smaller pixel density). C. Projection of maximum pixel intensity at each pixel across all 1260 images showing the positions occupied by the larvae across time. The red circle indicates the well for which data are shown in D and E. D. Distance traveled between successive video frames (1 second intervals) across 20 minutes of spontaneous activity recording followed by a 1 minute dark flash trial. The saw-tooth pattern indicates the larvae swimming in typical discrete bouts separated by rest periods. Activity during dark flash does not appear to be elevated over baseline on this trial. E. The data acquired for each behavior recording trial.

Results

Spontaneous Calcium Dynamics

Hypothesis 1 stated that drug type would have similar effects on the amplitude of calcium signaling, but the dose would increase the amplitude of the calcium oscillations. Data were analyzed using a repeated measures ANOVA with dose (control, low, medium, high) as the within-subjects factor and drug type (caffeine, paraxanthine) as the between subjects factor. Mauchly's test indicated that the assumption of sphericity for dose has been violated, $X^2 = 11.77$, $p = .039$, so the degrees of freedom were corrected using Greenhouse-Geisser estimates of sphericity ($\varepsilon = .665$). Calcium oscillation amplitude was not significantly affected by drug type, $F(1, 12) = 0.161$, $p = .695$, partial $\eta^2 = .013$, when amplitude was examined across all frequencies. Caffeine ($n = 7$) and paraxanthine ($n = 7$) had the same effect on amplitude. Drug dose did not affect calcium oscillation amplitude, $F(1.995, 23.94) = 0.484$, $p = .622$, partial $\eta^2 = .039$, when amplitude was examined across all frequencies. All the doses ($n = 12$ in each group) administered had no effect on calcium signaling.

I performed a secondary analysis examining how drug type and dose affected each of the frequency bins separately to better understand the effects of dose and drug type at individual frequencies. The data were analyzed using repeated measures ANOVA with dose (control, low, medium, high) and frequency bin (0.001 – 0.01 Hz, 0.01 – 0.05 Hz, 0.05 – 0.1 Hz, 0.1 – 1 Hz, 1-2.5 Hz) as the within-subjects factors and drug type (caffeine, paraxanthine) as the between-subjects factor. Mauchly's test indicated that the assumption of sphericity for frequency has been violated, $X^2 = 204.046$, $p < .001$, so the

degrees of freedom were corrected using Greenhouse-Geisser estimates of sphericity (ε = .319). There were no significant effects of drug dose on amplitude at any frequency bin (bin 1, $F(0.957, 11.484) = 0.173$, $p = .873$, partial $\eta^2 = .014$; bin 2, $F(0.957, 11.484) = 1.311$, $p = .28$, partial $\eta^2 = .098$; bin 3, $F(0.957, 11.484) = 2.056$, $p = .25$, partial $\eta^2 = .108$; bin 4, $F(0.957, 11.484) = 2.089$, $p = .137$, partial $\eta^2 = .148$; & bin 5, $F(0.957, 11.484) = 0.827$, $p = .453$, partial $\eta^2 = .065$).

Drug type also had no effect on amplitude at any frequency bin (bin 1, $F(1, 12) = 0.052$, $p = .823$, partial $\eta^2 = .004$; bin 2, $F(1, 12) = 1.957$, $p = .145$, partial $\eta^2 = .140$; bin 3, $F(1, 12) = 1.451$, $p = .25$, partial $\eta^2 = .108$; bin 4, $F(1, 12) = 0.731$, $p = .415$, partial $\eta^2 = .056$; & bin 5, $F(1, 12) = .381$, $p = .548$, partial $\eta^2 = .031$). Caffeine and paraxanthine had the same effects on amplitude within each of the frequency bins.

There were no interactions between drug type and dose, (bin 1, $F(3, 432) = 1.698$, $p = .873$, partial $\eta^2 = .014$; bin 2, $F(3, 432) = 1.752$, $p = .204$, partial $\eta^2 = .127$; bin 3, $F(3, 432) = 1.520$, $p = .237$, partial $\eta^2 = .112$; bin 4, $F(3, 432) = 0.091$, $p = .530$, partial $\eta^2 = .054$; & bin 5, $F(3, 432) = 0.733$, $p = .496$, partial $\eta^2 = .054$). Drug type affected the amplitude within each of the frequency bins in the same way at each of the doses administered. This is important to report as a significant interaction would suggest caffeine and paraxanthine influence calcium signaling differently.

Evoked Calcium Response

The data were analyzed using repeated measures ANOVA with dose (control, low, medium, high) as the within-subjects factor and drug type (caffeine, paraxanthine) as the between-subjects factor. Mauchly's test indicated that the assumption of sphericity

for dose has not been violated, X 2 = 6.143, p = .294. Drug type did not affect the average percent change in fluorescence (ΔF), F(1, 12) = 1.657, p = .222, partial η2 = .121. This supports our hypothesis and suggests that caffeine and paraxanthine affected Ca2+ signaling in the same way. Hypothesis 2 stated that as dose increase, there would be an increased percent change in calcium fluorescence. Dose did not affect the average ΔF, F(3, 36) = 0.729, p = .503, partial η2 = .057. This indicates that dose did not have an effect on Ca2+ signaling. There was not a significant interaction between drug type and dose on average ΔF, F(3, 432) = 0.056, p = .982, partial η2 = .005. The interaction between dose and drug type met the assumptions for sphericity. The interaction is important to report since it provides information supporting there were no differences across the average ΔF based on the drug or dose administered.

Hypothesis 2c states that there should be a similar response index between the drug types tested. The data were analyzed using repeated measures ANOVA with dose (control, low, medium, high) as the within-subjects factor and drug type (caffeine, paraxanthine) as the between-subjects factor. Mauchly's test indicated that the assumption of sphericity for dose has been violated, X 2 = 21.560, p = .001, so the degrees of freedom were corrected using Greenhouse-Geisser estimates of sphericity (ε = .459). Drug type did not significantly affect the response index of the neurons, F(1, 7) = 0.162, p = .700, partial η2 = .023. Caffeine and paraxanthine had the same effect on the response index for Ca2+ signaling after the visually-evoked stimulus. Hypothesis 2 states that dose should increase the response index. Dose did not have any effect on the

response index, F(1.377, 9.639) = 0.168, p = .792, partial η2 = .023. Increasing dose did not affect the calcium response after the visually-evoked stimulus. Dose and drug type had no interactions effect on the response index, F(1.377, 67.473) = 0.636, p = .508, partial η2 = .083. This supports the idea that caffeine and paraxanthine have similar effects on Ca2+ signaling within the neuron. Hypothesis 2 states that drug type will produce a similar slope for Ca2+ response after the dimming stimulus.

Spontaneous Locomotor Behavior

Hypothesis 4 states that drug type will not affect evoked swimming behaviors; however, the dose will decrease spontaneous swimming behaviors. The primary analysis investigated swimming behaviors across the 20-minute recording block. The data were analyzed using repeated measures ANOVA with dose (control, low, medium, high) as the within-subjects factor and drug type (caffeine, paraxanthine) as the between-subjects factor. Mauchly's test indicated that the assumption of sphericity for dose for total distance has been violated, $X^2 = 11.435$, $p = .045$, so the degrees of freedom were corrected using Greenhouse-Geisser estimates of sphericity ($\varepsilon = .598$). Drug type did not affect the total distance traveled across the 20 minute recording period, $F(1, 10) = 0.070$, $p = .797$, partial $\eta^2 = .007$. Administration of caffeine or paraxanthine did not change the total distance swam. Dose did not affect the total distance traveled across the 20-minute recording period, $F(1.794, 17.942) = 1.142$, $p = .336$, partial $\eta^2 = .103$. Increasing dose did not have an effect on the total distance swam. There was no interaction between dose and drug type, $F(1.794, 179.42) = 0685$, $p = .336$, partial $\eta^2 = .064$. Caffeine and paraxanthine affected the total distance swam in the same way across all the doses tested.

Mauchly's test indicated that the assumption of sphericity for dose for average speed has been violated, $X^2 = 12.184$, $p = .033$, so the degrees of freedom were corrected using Greenhouse-Geisser estimates of sphericity ($\varepsilon = .596$). Drug type did not affect the average speed swam across the 20-minute recording period, $F(1, 10) = .018$, $p = .897$, partial $\eta^2 = .737$. Administration of caffeine and paraxanthine affected the average speed swam in the same way. Dose did not affect the average speed swam across the 20-minute recording period, $F(1.787, 17.867) = 1.335$, $p = .285$, partial $\eta^2 = .118$. Increasing the dose did not change the average speed the zebrafish swam. Drug type and dose did not have an interaction, $F(1.787, 178.67) = 0.881$, $p = 420$, partial $\eta^2 = .081$. Caffeine and paraxanthine affected the average speed swam across all the doses tested.

Mauchly's test indicated that the assumption of sphericity for dose for maximum speed has been met, $X^2 = 10.206$, $p = .071$, so the degrees of freedom were not corrected. Drug type did not affect the maximum speed swam, $F(1, 10) = 0.052$, $p = .824$, partial $\eta^2 = .005$. Caffeine and paraxanthine did not affect the maximum speed recorded during the 20-minute recording block. Dose did not affect the maximum speed, $F(3, 30) = 2.301$, $p = .097$, partial $\eta^2 = .187$. Increasing doses had not effect on the maximum speed recorded during the 20-minute recording block. There was not interaction between drug type and dose, $F(3, 300) = 0.258$, $p = .855$, partial $\eta^2 = .025$. Caffeine and paraxanthine affected the maximum speed across all the doses tested.

A secondary analysis was performed to examine the effects of drug type and dose on swimming behaviors on individual time bins that broke up the 20-minute recording period into four 5-minute time bins. This allowed us to more closely examine potential differences in metabolism rates across varying doses. The data were analyzed using repeated measures ANOVA with dose (control, low, medium, high) and time bin (1 – 5, 6 – 10, 11 – 15, 16 – 20 minutes) as the within-subjects factors and drug type (caffeine, paraxanthine) as the between-subjects factor. Mauchly's test indicated that the assumption of sphericity for dose for total distance has been violated, $X^2 = 11.540$, $p = .043$, so the degrees of freedom were corrected using Greenhouse-Geisser estimates of sphericity ($\varepsilon = .613$). Mauchly's test indicated that the assumption of sphericity for time bin for total distance has been violated, $X^2 = 12.615$, $p = .028$, so the degrees of freedom were corrected using Greenhouse-Geisser estimates of sphericity ($\varepsilon = .595$). Table 3 shows drug type did not affect total distance traveled, $F(1, 10) = 0.003$, $p = .957$, partial $\eta^2 = .000$. Caffeine and paraxanthine affected the total distance swam in the same way. Dose did not affect the total distance traveled, $F(1.840, 18.401) = 1.178$, $p = .335$, partial $\eta^2 = .105$. Table 4 shows the varying doses administered had not effects on how far the fish swam throughout each of the time bins. Table 5 shows time bin had not effect on the total distance swam, $F(1.784, 17.844) = 0.183$, $p = .907$, partial $\eta^2 = .018$. There were no differences in the total distance swam throughout the time bins. There was no interaction between drug type and dose on the total distance swam, $F(1.840, 184.01) = 1.126$, $p = .341$, partial $\eta^2 = .101$. Caffeine and paraxanthine affected the total distance swam in the same way at each of the varying doses.

Mauchly's test indicated that the assumption of sphericity for dose for average speed has been violated, $X^2 = 11.611$, $p = .042$, so the degrees of freedom were corrected using Greenhouse-Geisser estimates of sphericity ($\varepsilon = .612$). Mauchly's test indicated that the assumption of sphericity for time bin for average speed has been violated, $x^2 = 12.273$, $p = .032$, so the degrees of freedom were corrected using Greenhouse-Geisser estimates of sphericity ($\varepsilon = .597$). Drug type did not affect the average swimming speed throughout the time bins, $F(1, 10) = 0.003$, $p = .960$, partial $\eta^2 = .000$. Caffeine and paraxanthine did not have an effect on the average speed swam (Table 3). Dose did not affect the average speed swam, $F(1.837, 18.371) = 1.172$, $p = .328$, partial $\eta^2 = .105$ (Table 4). Time bin did not affect the average speed swam, $F(1.792, 17.919) = 0.151$, $p = .839$, partial $\eta^2 = .839$. Table 5 shows the average speed remained the same throughout the time bins. There was no interaction between drug type and dose, $F(1.837, 183.71) = 1.123$, $p = .342$, partial $\eta^2 = .101$. Caffeine and paraxanthine affected the average speed swam in the same way at each of the varying doses

Mauchly's test indicated that the assumption of sphericity for dose for maximum speed has been violated, $X^2 = 11.741$, $p = .040$, so the degrees of freedom were corrected using Greenhouse-Geisser estimates of sphericity ($\varepsilon = .580$). Mauchly's test indicated that the assumption of sphericity for time bin for maximum speed has been met, $X^2 = 7.999$, $p = .159$. Drug type did not affect the maximum speed swam $F(1, 10) = 3.024$, $p = .113$, partial $\eta^2 = .232$. Table 3 shows administration of caffeine or paraxanthine did not affect swimming speed. Dose did not affect the maximum swimming speed, $F(1.740, 17.404) = 1.669$, $p = .218$, partial $\eta^2 = .143$ (Table 4). Time bin had no effect on the

maximum speed swam, $F(2.101, 21.008) = 0.774$, $p = 480$, partial $\eta^2 = .072$. There were no differences in the maximum speed swam across the time bins (Table 5). There was no interaction between drug type and dose, $F(1.740, 174.04) = 0.976$, $p = .417$, partial $\eta^2 = .089$. Caffeine and paraxanthine produced the same results on maximum speed throughout the varying doses.

Table 3

Effects of drug type on behavioral trials

	Caffeine			Paraxanthine		
Spontaneous	*n*	*M(SD)*	95% CI	*n*	*M(SD)*	95% CI
Total Distance (mm)	6	365.8 (135.5)	[-283.9, 298.2]	6	358.7 (289.9)	[298.2, -283.9]
Average Speed (mm/s)	6	1.2 (0.6)	[0.5, 1.9]	6	1.2 (1.0)	[0.5, 1.9]
Max Speed (mm/s)	6	13.7 (2.0)	[10.7, 16.6]	6	10.4 (4.1)	[7.5, 13.4]
Evoked						
Total Distance (mm)	6	60.7 (33.7)	[38.9, 84.6]	6	101.6 (43.2)	[77.7, 125.4]
Average Speed (mm/s)	6	1.0 (0.6)	[0.6, 1.4]	6	1.7 (0.7)	[1.3, 2.1]
Max Speed (mm/s)	6	6.1 (1.7)	[3.4, 8.9]	6	8.9 (3.9)	[6.2, 11.6]

*Note. *p< .05 for F test; CI = Confidence Interval around mean differences*

Table 4

Effect of dose on behavioral trials

	Control			Low			Med			High		
Spontaneous	*n*	*M(SD)*	95% CI	*n*	*M(SD)*	95% CI	*n*	*M(SD)*	95% CI	*n*	*M(SD)*	95% CI
Total Distance (mm)	6	390.8 (294.1)	[192.7, 588.8]	6	438.4 (360.1)	[199.9, 676.9]	6	368.3 (371.4)	[129.8, 606.8]	6	251.6 (163.8)	[144.9, 358.2]
Average Speed (mm/s)	6	1.3 (1.0)	[0.6, 2.0]	6	1.5 (1.2)	[0.7, 2.3]	6	1.2 (1.3)	[0.4, 2.0]	6	0.9 (0.5)	[0.5, 1.2]
Max Speed (mm/s)	6	11.5 (7.1)	[6.8, 16.3]	6	13.6 (7.3)	[9.4, 17.8]	6	13.7 (4.4)	[10.8, 16.7]	6	9.3 (4.3)	[6.8, 11.8]
Evoked												
Total Distance (mm)	6	108.9 (30.9)	[96.6, 121.1]	6	74.2 (18.7)	[62.0, 86.3]	6	85.6 (56.5)	[53.6, 117.7]	6	55.9 (44.6)	[30.9, 80.8]
Average Speed (mm/s)	6	1.8 (0.5)	[1.6, 2.0]	6	1.2 (0.3)	[1.0, 1.4]	6	1.4 (0.9)*	[0.9, 1.9]	6	0.9 (0.7)	[0.5, 1.3]
Max Speed (mm/s)	6	7.0 (2.9)	[5.4, 8.7]	6	8.4 (4.1)	[5.7, 11.1]	6	8.0 (6.5)	[3.9, 12.2]	6	6.7 (7.7)	[1.8, 11.5]

*Note: *p< .05 for F test; CI = confidence interval around mean differences*

Table 5

Effects of time bin on behavioral trials

	Time Bin 1			Time Bin 2			Time Bin 3			Time Bin 4		
Spontaneous	*n*	*M(SD)*	95% CI	*n*	*M(SD)*	95% CI	*n*	*M(SD)*	95% CI	*n*	*M(SD)*	95% CI
Total Distance (mm)	6	350.6 (192.6)	[220.7, 480.4]	6	363.6 (242.2)	[200.3, 527.0]	6	360.3 (185.6)	[238.0, 482.6]	6	374.5 (276.6)	[189.6, 559.4]
Average Speed (mm/s)	6	1.2 (0.6)	[07.3, 1.6]	6	1.2 (0.8)	[0.7, 1.8]	6	1.2 (0.6)	[0.8, 1.6]	6	1.2 (0.9)	[0.6, 1.9]
Max Speed (mm/s)	6	11.9 (4.6)	[9.1, 14.7]	6	11.1 (4.2)	[8.6, 13.7]	6	12.3 (4.2)	[9.8, 14.7]	6	12.9 (4.1)	[10.2, 15.7]

*Note: *p< .05 for F test; CI = confidence interval around mean differences*

Evoked Locomotor Behavior

The data were analyzed using repeated measures ANOVA with dose (control, low, medium, high) as the within-subjects factor and drug type (caffeine, paraxanthine) as the between-subjects factor. Mauchly's test indicated that the assumption of sphericity for dose has been met for total distance, X2 = 7.033, p = .221; for average speed, X2 = 7.033, p = .221; and for maximum speed, X2 = 6.725, p = .244.

In contrast to spontaneous swimming, Table 3 shows drug treatments did influence evoked swimming in the light dimming startle assay. There was a main effect of drug type on swimming distance in the 20 seconds following light dimming, F(1, 10) = 7.286, p = .022, partial η2 = .422, 95% CI of the mean differences[74.581, 7.131], with the Bonferroni pairwise comparison showing caffeine treated larvae swam significantly less than paraxanthine treated larvae (M = 60.711, SD = 33.710 and M = 101.567 SD = 43.150 mm distance for caffeine and paraxanthine groups, respectively). Drug type also affected average swimming speed during startle, F(1, 10) = 7.286, p = .022, partial η2 = .422, 95% CI of the mean differences [1.213, 0.119], with the Bonferroni pairwise comparison test showing caffeine treated larvae swimming significantly slower than paraxanthine treated larvae (M = 1.012 SD = 0.562 and M = 1.693, SD = 0.719 mm/s respectively) The maximum speed reached was not affected by drug type, F(1, 10) = 2.499, p = .145, partial η2 = .200.

There was a main effect of drug dose for total distance swam during startle swimming, $F(3, 30) = 9.049$, $p < .001$, partial $\eta^2 = .475$. The Bonferroni pairwise

comparisons of dose was significant showing the control group (*M* = 108.9, *SD* = 30.9) swam further than the low dose group (*M* = 74.2, *SD* = 18.7) with a 95% CI[16.846, 52.550] and the high dose group (*M* = 55.9, *SD* = 44.6) with a 95% CI[22.253, 83.788].

Table 5 shows the average distance swam for each of the doses and the corresponding confidence intervals. There was no significant interaction between the drug dose administered and time bin for maximum speed, $F(3.945, 39.447) = 3.044$, $p = .233$, partial $\eta^2 = .233$. *Figure 8* shows the maximum speed across the different doses and time bin.

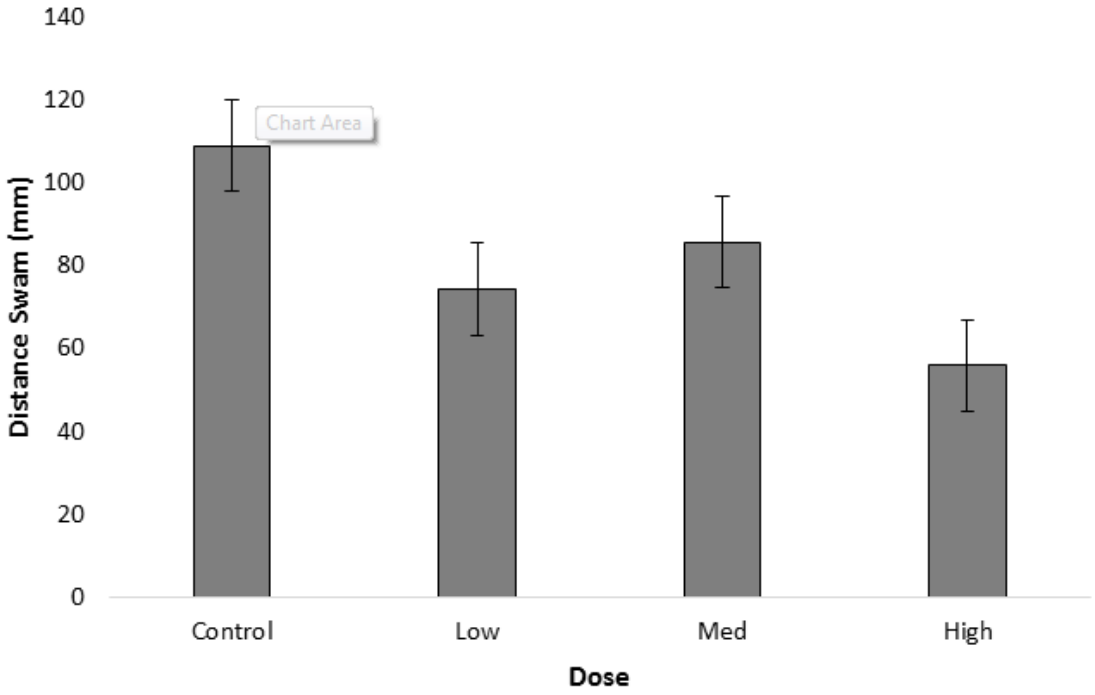

Figure 19. Startle swimming behaviors categorized by dose received. Control (no drug); Low (Caff:50μM/PX:40μM); Med (Caff:125μM/PX:100μM); High (Caff:250μM/PX:200μM). Error bars represent the standard error of the mean.

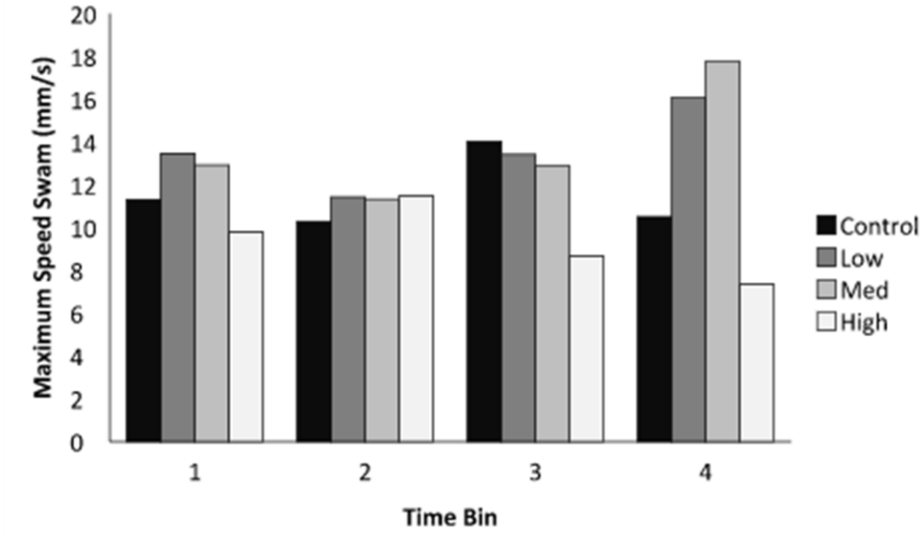

Figure 22. Maximum swimming speed (mm/s) categorized by dose received. Control (no drug); Low (Caff:50μM/PX:40μM); Med (Caff:125μM/PX:100μM); High (Caff:250μM/PX:200μM)

Heart Rate Analysis

Hypothesis 3 suggests that heart rate will be increased by both drug type and dose. The data were analyzed using repeated measures ANOVA with dose (control, low, medium, high) as the within-subjects factor and drug type (caffeine, paraxanthine) as the between-subjects factor. Mauchly's test indicated that the assumption of sphericity for dose has been met, $X^2 = 4.654$, $p = .462$. Drug type had no effect on heart rate, $F(1, 11) = 0.838$, $p = .380$, partial $\eta^2 = .071$. Caffeine ($n = 7$) and paraxanthine ($n = 6$) had the same effects on heart rate. Figure 9 shows dose had a significant effect on heart rate (bps), $F(3, 33) = 11.187$, $p < .001$, partial $\eta^2 = .504$. The Bonferroni pairwise comparisons of heart rate was significant showing the control group ($M = 1.75$, $SD = 0.442$ bps) was significantly higher than the low dose group ($M = 1.36$, $SD = 0.230$ bps) with a 95% CI[0.101, 0.674] and the medium dose group ($M = 1.76$, $SD = 0.270$ bps) with a 95% CI[0.192, 0.956]. *Figure 9* shows the control group had the highest heart rate, $M = 1.750$, $SD = 0.442$, the low dose group had the second highest heart rate, $M = 1.364$, $SD = 0.230$, followed by the highest dose group, $M = 1.349$, $SD = 0.298$, and the medium dose group had the lowest heart rate, $M = 1.176$, $SD = 0.270$. There was no interaction between drug type and dose received on heart rate, $F(3, 363) = 0.060$, $p = .980$, partial $\eta^2 = .005$. Caffeine and paraxanthine produced the same results across all doses tested.

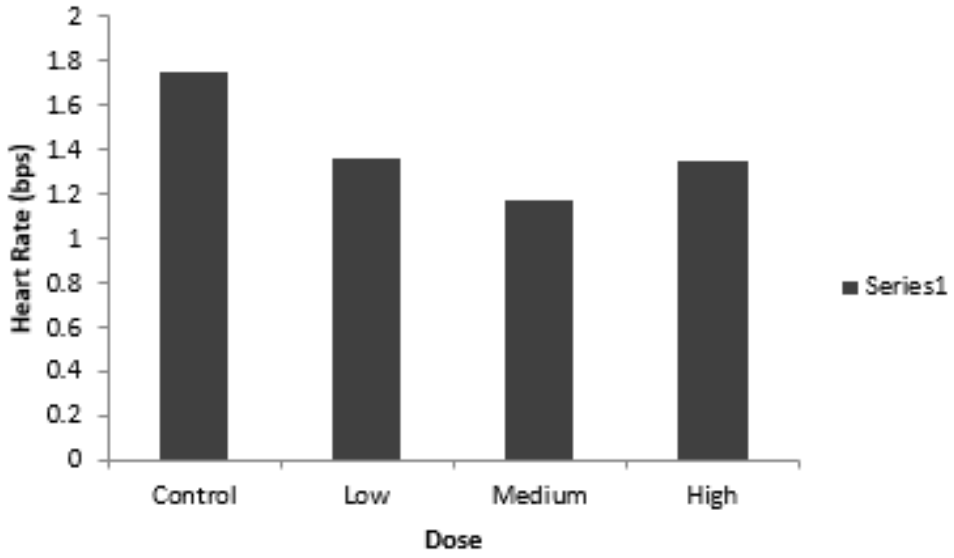

Figure 25. Shows the average heart rate in beats per second (bps) sorted by dose received.

Discussion

These experiments were intended to provide information about effects of caffeine and paraxanthine on intracellular Ca^{2+} and behavior in an important animal model system, zebrafish larvae. The lack of consistent or hypothesized caffeine and paraxanthine effects suggest that the dose range I used may have been too low to produce the intended effects *in vivo* within zebrafish larvae. Prior experiments investigating the effects of caffeine and paraxanthine used much larger doses, for example, Ladu et al. (2015) exposed larval zebrafish to 0.257 mM caffeine, whereas the highest concentration used in the current study was 250μM. Guerreiro et al., (2008) tested the neuroprotective qualities exposed cell cultures to 25 mM. However, it had been suggested lower doses would be able to achieve the same effects while testing the effects of these drugs *in vivo* on intracellular calcium concentrations (Guerreiro et al., 2008). The doses used were estimates based on prior caffeine research in zebrafish models in which the zebrafish were expected to survive several days past drug administration (Abdelkader et al., 2013).

Prior research suggests exposure to caffeine or paraxanthine results in an increase of intracellular calcium concentrations via activation of ryanodine receptors (Guerreiro et al., 2008). Per hypothesis 1, I expected to see a main effect across the doses, as an increase in dose should result in changes in Ca^{2+} signaling. Contradictory to my hypothesis and what the literature suggested, dose did not affect the amplitude of the calcium oscillations. The concentrations were estimated based on prior research demonstrating the effects of caffeine administration in which the zebrafish also survived 72 hours post-administration (Abdelkader et al., 2013). The last point is important

because I chose a dose range that would be applicable in neuroprotection studies, so I wanted to avoid toxic concentrations. Ryanodine receptors release Ca^{2+} in a bell-shaped dose-dependent fashion, with the receptors only activating the Ca^{2+} release channels in the intermediate range (Bezprozvanny et al., 1991; Fill & Copello, 2002; Verkhratsky, 2006). It was expected that the dose administered would influence the frequency or amplitude of Ca^{2+} oscillations (Berridge et al., 2000, Cheng et al., 1993). However, the dose of caffeine or paraxanthine showed no effect on the frequency or amplitude of Ca^{2+} oscillations. It is possible the concentration of caffeine or paraxathine was either too low or too high to activate the Ca^{2+} release channels resulting in changes in intracellular Ca^{2+} concentration or affect Ca^{2+} oscillations.

The literature suggests ryanodine receptors affect Ca^{2+} signaling by affecting the FM encoding of the Ca^{2+} signal. I broke down the ranges of frequencies measured into five bins (0.001 – 0.01 Hz, 0.01 – 0.05 Hz, 0.05 – 0.1 Hz, 0.1 – 1 Hz, 1-2.5 Hz) to assess drug effects on Ca^{2+} oscillations resulting at each individual frequency bin. I did not expect to see a main effect of drug type within the frequency bins. The results are congruent with the expectation there would be no main effect for drug type, per hypothesis 1 This is supportive to the claim that caffeine and paraxanthine have similar effects on Ca^{2+} signaling, specifically the amplitude of the frequencies. It was anticipated the changes in dose would impact Ca^{2+} oscillations, per hypothesis 1. The results did not coincide with the literature suggesting administration of caffeine or paraxanthine would result in increases of intracellular Ca^{2+} concentrations through activation of ryanodine receptors (Guerreiro et al., 2008).

There were several limitations affecting the analysis of spontaneous Ca^{2+} dynamics. Firstly, I created the ROIs surrounding the entire neuron cluster, rather than around the individual neurons forming the cluster. If the individual cells creating the cluster were oscillating at different times, the ROIs I used would not have been able to detect the changes. Using several smaller ROIs within each cluster may have allowed the detection of changes in the oscillations. Second, the imaging speed used (5 Hz) could have also prevented detection of any frequencies above 2.5 Hz. The GCaMP transgenic line has been recorded to respond up to at least 20 Hz (Kim & Ziff, 2014). There may have been effects on higher frequencies; however, the parameters used to record the neurons would not have been able to capture these effects, thus restricting the analysis to frequencies 2.5 Hz and below.

Previous research has not explored changes in intracellular calcium concentrations linked to caffeine administration within the zebrafish. Paraxanthine administration to the zebrafish has not been documented within the literature. However, previous studies of intracellular calcium release channels suggest administration of caffeine or paraxanthine should produce an increase in intracellular calcium levels after a stimulus (Grienberger et al., 2012; Fill & Copello, 2013). Since ryanodine receptors release Ca^{2+} in a dose-dependent bell-shaped curve, it's possible the doses used could have been either too low or too high. My results are not congruent with current literature, as the trails receiving different doses were similar to the control group. This suggests the doses administered may not have been within the correct range to produce the intended effects. There were no difference between caffeine and paraxanthine administration. This

coincides with the hypothesized outcome, however, since neither drug showed significant effects relative to the pre-drug control condition, it is impossible to interpret the lack of a main effect of drug type as evidence that the two drugs have equivalent physiological actions.

Prior research suggests caffeine exposure increases the heart rate in zebrafish (Abdelkader et al., 2013). The 200μM dose of caffeine did significantly affect the heart rate of the zebrafish. The current literature states the average resting heart rate in a zebrafish embryo is 2.16 bps (Burns et al., 2005). The control group, averaging at 1.75 bps, has a lower average resting heart rate than what the literature suggest. The literature states embryos exposed to doses of caffeine above 100 μM significantly increases heart rate over control groups (Abdelkader et al, 2013). My results do not coincide with current literature, as the control condition in the current study had the highest heart rate, an opposite of caffeine from what has been previously reported . One possibility that could explain this is that heart rate was measured 4 times across 104 minutes in the current study, and the duration of restraint and exposure to the imaging laser may have led to a lower heart rate as part of general fatigue response to the experiment. However, none of the larvae died during calcium imaging and all were successfully de-embedded afterwards.

The differences in spontaneous swimming behaviors attributed to change in dose of the zebrafish post treatment were not consistent with previous reports (Holtzman, 1989; Ladu et al., 2015). Acute caffeine exposure was shown to decrease active voluntary behaviors, including spontaneous swimming behaviors, in a dose dependent fashion, in

two separate studies (Holtzman, 1989; Ladu et al., 2015). However, I saw no significant differences between the total distance traveled, average speed, or the minimum speed during the 20 minute time bin across the four doses tested in this experiment. Doses of caffeine under 100 µM do not produce changes in swimming behaviors (Abdelkader et al., 2013; Capiotti et al., 2011). Since paraxanthine is the main metabolite of caffeine, I assumed that there would be no changes in swimming behavior after exposure to 80 µM of paraxanthine. As the low dose conditions for caffeine and paraxanthine was less than the aforementioned concentrations, my results for the low dose condition are congruent with previous research as the low dose group was not significantly different from the control group.

I broke up the 20 minute time bin into four sets of 5 minute time bins to more closely examine the effects possibility that drug effects change over time within each 20 minute behavior recording. There were no significant differences in voluntary swimming behaviors across the time bins. However, there was a significant interaction between the dose and time bin. This interaction suggests the varying doses may influence the speed the zebrafish metabolizes caffeine and paraxanthine.

By using a metabolically equivalent ratio of paraxanthine to caffeine, I did not expect to see any main effects of drug type in the analysis. My results were consistent with our hypothesis as there were no discernible differences between the groups treated with caffeine or paraxanthine. To some extent these results support the suggestion that caffeine and paraxanthine affect the same receptors to produce similar behaviors.

However, as mentioned previously, the lack of significant different across drug dosages limits any interpretations of these results.

One clear limiation to my experimental design was that time and drug dosage were confounded, since drugs were given as progressively higher concentrations over time and measurements were made repeatedly. I was unable to counterbalance the doses administered during this experiment. It would have been difficult to ensure that the higher doses would have been fully flushed from the zebrafish's system before testing the lower doses. This makes it possible that other processes related to the passage of time or experimental procedures, including simple fatigue, may have influenced cellular or behavioral responses to the drugs. It is also possible that prolonged exposure to affected results, for example, if previous exposure to lower doses bunted the responses to higher doses through a type of tolerance or habituation mechanism.

Future research is needed to provide further understanding of the effects caffeine and paraxanthine on Ca^{2+} signaling. The next step would be to test a wider range of doses, which will provide information on the ideal dose to activate ryanodine receptors in order to affect intracellular Ca^{2+} concentrations. Increasing the imaging speed would allow researchers to analyze a broader range of frequencies to identify changes in Ca^{2+} oscillations this experiment was unable to assess due to the parameters of the Ca^{2+} imaging. To avoid confounds related to time and previous drug exposure, any follow up experiment should probably use a between subjects design in which animals receive only one exposure to the drug.

The neuroprotective effects of caffeine are supported by a numerous studies investigating the effects in humans, animal models, and in cell. Calcium, the most prominent signaling molecule within cells, is known to have a role in inducing apoptosis. Several studies have linked PD-related DA death to complications with calcium. The neuroprotective qualities of caffeine are attributed to its main metabolite paraxanthine which causes the release of calcium from the ER via ryanodine receptors. Although this study did not provide evidence caffeine's or paraxanthine's effect on intracellular calcium signaling, the literature still supports caffeine as a strong candidate for a potential therapeutic treatment in neurodegenerative diseases.

References

Abdelkader, T. S., Chang, S., Kim, T., Song, J., Kim, D. S., & Park, J. H. (2013). Exposure time to caffeine affects heartbeat and cell damage-related gene expression of zebrafish danio rerio embryos at early developmental stages. *Journal of Applied Toxicology, 33,* 1277-1283. doi: 10.1002/jat.2787

Amador, F. J., Stathopulos, P. B., Enomoto, M., & Ikura, M. (2013). Ryanodine receptor calcium release channels: Lessons from structure–function studies. *FEBS Journal, 280*, 5456-5470. doi: 10.1111/febs.12194

Arnaud, M. J. (2011). Pharmacokinetics and metabolism of natural methylxanthines in animal and man. In B. Fredholm (Eds). *Handbook of Experimental Pharmacology*, (pp. 33-91). Sweden: Springer.

Ahmad, F., Noldus, L. P., Tegelenbosch, R. A., & Richardson, M. K. (2012) Zebrafish embryos and larvae in behavioural assays. *Behaviour, 149,* 1241-1281. doi: 10.1163/156839X-00003020

Arrazola, M. S., Silva-Alvarez, C., & Inestrosa, N. C. (2015). How the wnt signaling pathway protects from neurodegeneration: The mitochondrial scenario. *Frontiers in Cellular Neuroscience, 9,* 166-178. doi:10.3389/fncel.2015.00166

Ascherio, A., Zhang, S. M., Hernán, M. A., Kawachi, I., Colditz, G. A., Speizer, F. E., & Willet, W. C. (2001). Prospective study of caffeine consumption and risk of

Parkinson's disease in men and women. *Annals of Neurology, 50*, 56-63. doi: 10.1002/ana.1052

Ashworth, R., & Bolsover, S. R. (2002). Spontaneous activity-independent intracellular calcium signals in the developing spinal cord of the zebrafish embryo. *Developmental Brain Research, 139*, 131-137. doi: 10.1016/S0165-3806(02)00538-2

Azarashvili, T., Stricker, R., & Reiser, G. (2010). The mitochondria permeability transition pore complex in the brain with interacting proteins - promising targets for protection in neurodegenerative diseases. *Biological Chemistry, 391*, 619-629. doi: 10.1515/bc.2010.070

Benabid, A. L., Chabardes, S., Mitrofanis, J., & Pollak, P. (2009). Deep brain stimulation of the subthalamic nucleus for the treatment of Parkinson's disease. *Lancet Neurology, 8*, 67-81. doi: 10.5580/2c90

Benowitz, N. L., Jacob, P., Mayan, H., & Denaro, C. (1995). Sympathomimetic effects of paraxanthine and caffeine in humans. *Clinical Pharmacology Theory, 58*, 684-691. doi: 10.1016/0009-9236(95)90025-X

Berridge, M., Lipp, P., & Bootman, M. D. (2000). The versatility and universality of calcium signaling. *Nature Reviews Molecular Cell Biology, 1*, 11-21. doi: 10.1038/35036035

Bezprozvanny, I., Watras, J., & Ehrlich, B. E. (1991). Bell-shaped calcium-response curves of Ins(1, 4, 5)P3- and calcium-gated channels from endoplasmic reticulum of cerebellum. *Nature, 351,* 751-754. doi: 10.1038/351751a0

Blaustein, M. P., & Golovina, V. A. (2001). Structural complexity and functional diversity of endoplasmic reticulum ca2+ stores. *Trends in Neurosciences*, *24*, 602-608. doi: 10.1016/S0166-2236(00)01891-9

Bonati, M., Latini, R., Galletti, F., Young, J. F., Tognoni, G., & Garattini, S. (1982). Caffeine disposition after oral doses. *Clinical Pharmacology and Therapeutics*, *32*, 98-106. doi: 10.1038/clpt.1982.132

Brose, N., Petrenko, A. G., Sudhof, T. C., & Jahn, R. (1992). Synaptotagmin: A calcium sensor on the synaptic vesicle surface. *Science*, *256*, 1021-1025. doi: 10.1126/science.1589771

Burke, W. J., Li, S. W., Williams, E. A., Nonneman, R., & Zahm, D. (2003). 3,4-dihydroxyphenylacetaldehyde is the toxic dopamine metabolite in vivo: Implications for Parkinson's disease pathogenesis. *Brain Research*, *989*, 205-213. doi: 10.1016/S0006-8993(03)03354-7

Burke, W. J., Li, S. W., Chung, H. D., Ruggiero, D. A., Kristal, B. S., Johnson, E. M., … Zahm, D. S. (2004). Neurotoxicity of mao metabolites of catecholamine neurotransmitters: Role in neurodegenerative diseases. *Neurotoxicology*, *25*, 101-115. doi:10.1016/S0161-813X(03)00090-1

Burns, C. G., Milan, D. J., Grande, E. J., Rottbauer, W., MacRae, C. A., & Fishman, M. C. (2005). High-throughput assay for small molecules that modulate zebrafish embryonic heart rate. *Nature Chemical Biology*, *1*, 263-264. doi: 10.1038/nchembio732

Cali, T., Ottolini, D., & Brini, M. (2014). Calcium signaling in Parkinson's disease. *Cell and Tissue Research, 357*, 439-454. doi: 10.1007/s00441-014-1866-0

Capiotti, K. M., Menezes, F. P., Nazario, L. R., Pohlmann, J. B., de Oliveira, G. M., Fazenda, L., … Da Silva, R. S. (2011). Early exposure to caffeine affects gene expression of adenosine receptors, darpp-32 and bdnf without affecting sensibility and morphology of developing zebrafish (danio rerio). *Neurotoxicology and Teratology, 33*, 680-685. doi: 10.1016/j.ntt.2011.08.010

Cascarano, J., Montisano, D. F., Pickett, C. B., & James, T. W. (1982). Rough endoplasmic reticulum-mitochondrial complexes from rat liver. an extramitochondrial succinic dehydrogenase associated with this rough endoplasmic reticulum. *Experimental Cell Research, 139*, 39-50. doi: 10.1016/0014-4827(82)90316-0

Cesura, A. M., & Pletscher, A. (1992). The new generation of monoamine oxidase inhibitors. *Progress in Drug Research, 38*, 171-297. doi: 10.1007/978-3-0348-7141-9_3

Checkoway, H., Powers, K., Smith-Weller, T., Franklin, G. M., Longstreth, W. T., & Swanson, P. D. (2002). Parkinson's disease risks associated with cigarette smoking, alcohol consumption, and caffeine intake. *American Journal of Epidemiology, 155,* 732-738. doi: 10.1093/aje/155.8.732

Chen, J. F., Xu, K., Petzer, J. P., Staal, R., Xu, Y. H., Beilstein, M., … Schwarzschild, M. A. (2001). Neuroprotection by caffeine and a(2a) adenosine receptor inactivation in a model of Parkinson's disease. *The Journal of Neuroscience, 21,* RC143. doi: 10.1038/sj.bjp.0705185

Cheng, H., Lederer, W. J., & Cannell, M. B. (1993) Calcium Sparks: Elementary events underlying excitation-contraction coupling in heart muscles. *Science, 262,* 740-744. doi: 10.1126/science.8235594

Cools, R., Barker, R. A., Sahakian, B. J., & Robbins, T. W. (2003). L-dopa medication remediates cognitive inflexibility, but increases impulsivity in patients with Parkinson's disease. *Neuropsychologia, 41,* 1431-1441. doi: 10.1016/S0028-3932(03)00117-9

Copeland, D. E., & Dalton, A. J. (1959). An association between mitochondria and the endoplasmic reticulum in cells of the pseudobranch gland of a teleost. *The Journal of Biophysical and Biochemical Cytology, 5,* 393-396. doi: 10.1083/jcb.5.3.393.

De Pitta, M., Volman, V., Levine, H., & Ben-Jacob, E. (2009). Multimodal encoding in a simplified model of intracellular calcium signaling. *Cognitive Processing, 10*, 55-70. doi: 10.1007/s10339-008-0242-y

Denaro, C. P, Brown, C. R., Wilson, M., Jacob, P., & Benowitz, N. L. (1990). Dose-dependency of caffeine metabolism with repeated dosing. *Clinical Pharmacology and Therapeutics, 48*, 277-285. doi: 10.1038/clpt.1990.150

Dupont, G., Abou-Lovergne, A., & Laurent, C., (2008). Stochastic aspects of oscillatory Ca^{2+} dynamics in hepatocytes. *Biophysical Journal, 95,* 2196-2202. doi: 10.1529/biophysj.108.133777

Eriksen, J. L., Dawson, T. M., Dickson, D. W., & Petrucelli, L. (2003). Caught in the act: [alpha]-synuclein is the culprit in Parkinson's disease. *Neuron, 40*, 453-456. doi: 10.1201/9780203508596.sec3

Fearnley, J. M, & Lees, A. J. (1991). Ageing and Parkinson's disease: Substantia nigra regional selectivity. *Brain: A Journal of Neurology, 114*, 2283-2301. doi: 10.1093/brain/114.5.2283

Fill, M., & Copello, J. A. (2002). Ryanodine receptor calcium release channels. *Physiological Reviews, 82,* 893-922. doi: 10.1152/physrev.00013.2002

Filloux, F., & Townsend, J. J. (1993). Pre- and postsynaptic neurotoxic effects of dopamine demonstrated by intrastriatal injection. *Experimental Neurology, 119*, 79-88. doi: 10.1006/exnr.1993.1008

Fornai, F., Battaglia, G., Gesi, M., Giorgi, F. S., Orzi, F., Nicoletti, F., & Ruggieri, S. (2000). Time-course and dose-response study on the effects of chronic l-dopa administration on striatal dopamine levels and dopamine transporter following mptp toxicity. *Brain Research, 887,* 110-117. doi: 10.1016/S0006-8993(00)02999-1

Gahtan, E., Sankrithi, N., Campos, J. B., & O'Malley, D. M. (2002). Evidence for a widespread brain stem escape network in larval zebrafish. *Journal of Neurophysiology, 87,* 608-614. doi: 10.1152/jn.00596.2001

Grienberger, C. & Konnerth, A. (2012). Imaging calcium in neurons, *Neuron, 73,* 862-885. doi: 10.1016/j.neuron.2012.02.011

Grillner, P., & Mercuri, N. B. (2002). Intrinsic membrane properties and synaptic inputs regulating the firing activity of the dopamine neurons. *Behavioral Brain Research, 130,* 149-169. doi: 10.1016/S0166-4328(01)00418-1

Guerreiro, S., Toulorge, D., Hirsch, E., Marien, M., Sokoloff, P., & Michel, P. P. (2008). Paraxanthine, the primary metabolite of caffeine, provides protection against dopaminergic cell death via stimulation of ryanodine receptor channels. *Molecular Pharmacology, 74,* 980-989. doi: 10.1124/mol.108.048207

Holtzman, S. G. (1983). Complete, reversible, drug-specific tolerance to stimulation of locomotor activity by caffeine. *Life Sciences, 33,* 779-787. doi: 10.1016/0024-3205(83)90784-1

Hongpaisan, J., Winters, C. A., & Andrews, S. B. (2004). Strong calcium entry activates mitochondrial superoxide generation, upregulating kinase signaling in hippocampal neurons. *Journal of Neuroscience, 24*, 10878-10887. doi: 10.1523/JNEUROSCI.3278-04.2004

Hornykiewicz, O. (1993). Parkinson's disease and the adaptive capacity of the nigrostriatal dopamine system: Possible neurochemical mechanisms. *Advances in Neurology*, *60*, 140-147. Retrieved from: https://www.ncbi.nlm.nih.gov/pubmed/8420131

Hurley, M. J., & Dexter, D. T. (2012). Voltage-gated calcium channels and Parkinson's disease. *Pharmacology and Therapeutics, 133*, 324-333. doi: 10.1016/j.pharmthera.2011.11.006

Ichas, F., & Mazat, J. (1998). From calcium signaling to cell death: two conformations for the mitochondrial permeability transition pore. Switching from low- to high-conductance state. *Biochimica Et Biophysica Acta BBA - Bioenergetics, 1366*, 33-50. doi: 10.1016/S0005-2728(98)00119-4

Kalda, A., Yu, L., Oztas, E., & Chen, J. (2006). Novel neuroprotection by caffeine and adenosine a2a receptor antagonists in animal models of Parkinson's disease. *Journal of the Neurological Sciences, 248*, 9-15. doi: 10.1016/j.jns.2006.05.003

Kastanenka, K. V., Hou, S. S., Shakerdge, N., Logan, R., Feng, D., Susanna, W., … Bacskai, B. J. (2017). Optogenetic restoration of disrupted slow oscillations halts

amyloid deposition and restores calcium homeostasis in an animal model of alxheimer's disease. *PLoS ONE, 12*, e0170275. doi: 10.1371/journal.pone.0170275

Kim, S. & Ziff, E. B. (2014). Calciuneurin mediates synaptic scaling via synaptic trafficking of calcium-permeable AMPA receptors. *PLoS Biology, 12,* e10011900. doi: 10.1371/journal.pbio.1001900

Kinkhabwala, A., Riley, M., Koyama, M., Monen, J., Satou, C., Kimura, Y., … Fetcho, J. (2011). A structural and functional ground plan for neurons in the hindbrain of zebrafish. *Proceedings of the National Academy of Sciences of the United States of America, 108*, 1164-1169. doi: 10.1073/pnas.1012185108

Klein, C., & Westenberger, A. (2012). Genetics of Parkinson's disease. *Cold Spring Harbor Perspectives in Medicine*, *2*, a008888. doi: 10.1101/cshperspect.a008888

Kluck, R. M., Bossy-Wetzel, E., Green, D. R., & Newmeyer, D. D. (1997). The release of cytochrome c from mitochondria: A primary site for bcl-2 regulation of apoptosis. *Science, 275*, 1132-1136. doi: 10.1126/science.275.5303.1132

Kothakota, S., Azuma, T., Reinhard, C., Klippel, A., Tang, J., Chu, K., … Williams, L. T. (1997). Caspase-3-generated fragment of gelsolin: Effector of morphological change in apoptosis. *Science, 278*, 294-298. doi: 10.1126/science.278.5336.294

Kristal, B. S., Matsuda, M., & Byung, P. Y. (1996). Abnormalities in the mitochondrial permeability transition in diabetic rats. *Biochemical and Biophysical Research Communications, 222,* 519-523. doi: 10.006/bbra.1996.0776

Kristal, B. S., Conway, A. D., Brown, A. M, Jain, J. C., Ulluci, P. A., Li, S. W., & Burke, W. J. (2001). Selective dopaminergic vulnerability: 3, 4-dihydroxyphenylacetaldehyde targets mitochondria. *Free Radical Biology and Medicine, 30,* 924-931. doi: 10.1016/S0891-5849(01)00484-1

Ladu, F., Mwaffo, V., Li, J., Macri, S., & Porfiri, M. (2015). Acute caffeine administration affects zebrafish response to a robotic stimulus. *Behavioral Brain Research, 289,* 48-54. doi: 10.1016/j.bbr.2015.04.020

Lam, C. S., Korzh, V., & Strahle, U. (2005). Zebrafish embryos are susceptible to the dopaminergic neurotoxin MPTP. *European Journal of Neuroscience, 21,* 1758-1762. doi: 10.1111/j.1460-9568.2005.03988.x

Lamensdorf, I., Eisenhofer, G., Harvey-White, J., Hayakawa, Y., Kirk, K., & Kopin, I. J. (2000). Metabolic stress in pc12 cells induces the formation of the endogenous dopaminergic neurotoxin, 3, 4-dihydroxyphenylacetaldehyde. *Journal of Neuroscience Research, 60,* 552-558. doi: 10.1002/(SICI)1097-4547(20000515)60:4<552::AID-JNR14>3.0.CO;2-U

Lang, A. E., & Lozano, A. M. (1998). Parkinson's disease. First of two parts. *The New England Journal of Medicine*, *339*, 1044-1053. doi: 10.1056/NEJM199810083391506

Li, S. W., Lin, T. S., Minteer, S., & Burke, W. J. (2001). 3, 4-dihydroxyphenylacetaldehyde and hydrogen peroxide generate a hydroxyl radical: Possible role in Parkinson's disease pathogenesis. *Brain Research Molecular Brain Research*, *93*, 1-7. doi: 10.1016/S0169-328X(01)00120-6

Luo, Y., Hoffer, A., Hoffer, B., & Qi, X. (2015). Mitochondria: A therapeutic target for Parkinson's disease? *International Journal of Molecular Sciences*, *16*, 20704. doi: 10.3390/ijms160920704

Mannella, C. A., Buttle, K., Rath, B. K., & Marko, M. (1998). Electron microscopic tomography of rat-liver mitochondria and their interaction with the endoplasmic reticulum. *BioFactors*, *8*, 225-228. doi: 10.1002/biof.5520080309

Mattson, M. P. (2012). Parkinson's disease: Don't mess with calcium. *The Journal of Clinical Investigation*, *122*(4), 1195-1198. doi: 10.1172/jci62835

McCall, A. L., Millington, W. R., & Wurtman, R. J. (1982). Blood-brain barrier transport of caffeine: Dose-related restriction of adenine transport. *Life Sciences*, *31*, 2709-2715. doi: 10.1016/0024-3205(82)90715-9

McConkey, D. J., & Orrenius, S. (1997). The role of calcium in the regulation of apoptosis. *Biochemical and Biophysical Research Communications*, *239*, 357-366. doi: 10.1006/bbrc.1997.7409

McNeill, A., Wu, R., Tzen, K., Aguiar, P. C., Arbelo, J. M., Paolo, B., … Schapira, A. H. (2013). Dopaminergic neuronal imaging in genetic Parkinson's disease: Insights into pathogenesis. *PloS One*, *8*, e69190. doi:10.1371/journal.pone.0069190

Oldendorf, W. H. (1971). Brain uptake of radiolabeled amino acids, amines, and hexoses after arterial injection. *The American Journal of Physiology*, *221*, 1629-1639. doi: 10.3181/00379727-136-35270

Orrenius, S., Nicotera, P., & Zhivotovsky, B. (2003). Regulation of cell death: The calcium-apoptosis link. *Nature Reviews Molecular Cell Biology*, *4*, 552-565. doi: 10.1038/nrm1150

Panneton, W. M., Kumar, V. B., Gan, Q., Burke, W. J., & Galvin, J. E. (2010). The neurotoxicity of DOPAL: Behavioral and stereological evidence for its role in Parkinson disease pathogenesis. *PloS One*, *5*, e15251. doi: 10.1371/journal.pone.0015251.

Patergnani, S., Suski, J. M., Agnoletto, C., Bononi, A., Bonora, M., De Marchi, E., … Pinton, P. (2011). Calcium signaling around mitochondria associated membranes (MAMS). *Cell Communication and Signaling*, *9*, 19. doi: 10.1186/1478-811X-9-19

Polymeropoulos, M. H., Lavedan, C., Leroy, E., Ide, S. E., Dehejia, A., Dutra, A., … Nussbaum, R. L. (1997). Mutation in the alpha-synuclein gene identified in families with Parkinson's disease. *Science, 276*, 2045-2047. doi: 10.1126/science.276.5321.2045

Raturi, A., & Simmen, T. (2013). Where the endoplasmic reticulum and the mitochondrion tie the knot: The mitochondria-associated membrane (MAM). *Biochimica Et Biophysica Acta (BBA) - Molecular and Cell Biology of Lipids*, *1833*, 213-224. doi: 10.1016/j.bbamcr.2012.04.013

Rizzuto, R., Pinton, P., Ferrari, D., Chami, M., Szabadkai, G., Magalhaes, P. J., … Pozzan, T. (2003). Calcium and apoptosis: Facts and hypotheses. *Oncogene*, *22*, 8619-8627. doi: 10.1038/sj.onc.1207105

Rizzuto, R., De Stefani, D., Raffaello, A., & Mammucari, C. (2012). Mitochondria as sensors and regulators of calcium signalling. *Nature Reviews. Molecular Cell Biology*, *13*, 566-578. doi: 10.1038/nrm3412

Romano, S. A., Pietri, T., Perez-Schuster, V., Jouary, A., Haudrechy, M., & Sumbre, G. (2015). Spontaneous neuronal network dynamics reveal circuit's functional adaptations for behavior. *Neuron, 85*, 1070-1085. doi: 10.1016/j.neuron.2015.01.027

Scarlett, J. L., & Murphy, M. P. (1997). Release of apoptogenic proteins from the mitochondrial intermembrane space during the mitochondrial permeability transition. *FEBS Letters, 418*, 282-286. doi: 10.1016/S0014-5793(97)01391-4

Schapira, A. H., Cooper, J. M., Dexter, D., Jenner, P., Clark, J. B., & Marsden, C. D. (1990). Mitochondrial complex I deficiency in Parkinson's disease. *Journal of Neurochemistry, 54*, 823-827. doi: 10.1111/j.1471-4159.1990.tb02325.x

Smeyne, R. J., & Jackson-Lewis, V. (2005). The MPTP model of Parkinson's disease. *Molecular Brain Research, 134*, 57-66. doi: 10.1016/j.molbrainres.2004.09.017

Stefani, A., Lozano, A. M., Peppe, A., Stanzione, P., Galati, S., Tropepi, D., … Mazzone, P. (2007). Bilateral deep brain stimulation of the pedunculopontine and subthalamic nuclei in severe Parkinson's disease. *Brain: A Journal of Neurology, 130*, 1596-1607. doi: 10.1093/brain/awl346

Szalai, G., Krishnamurthy, R., & Hajnóczky, G. (1999). Apoptosis driven by ip3-linked mitochondrial calcium signals. *The EMBO Journal, 18*, 6349-6361. doi: 10.1093/emboj/18.22.6349

Szalai, G., Csordas, G., Hantash, B. M., Thomas, A. P., & Hajnoczky, G. (2000). Calcium signal transmission between ryanodine receptors and mitochondria. *Journal of Biological Chemistry, 275*, 15305-15313. doi: 10.1074/jbc.275.20.15305

Usachev, Y., Shmigol, A., Pronchuk, N., Kostyuk, P., & Verkhratsky, A. (1993). Caffeine-induced calcium release from internal stores in cultured rat sensory neurons. *Neuroscience*, *57*, 845. doi: 10.1016/0306-4522(93)90029-F

Verkhratsky, A. (2002). The endoplasmic reticulum as an integrating signalling organell: From neuron signalling to neuronal death. *European Journal of Pharmacology, 447*, 141-154. doi: 10.1016/S0014-2999(02)01838-1

Verkhratsky, A. (2006). Physiology and pathophysiology of the calcium store in the endoplasmic reticulum of neurons. *Physiological Reviews, 85*, 201-279. doi: 10.1152/physrev.00004.2004

Wallace, D. C. (1992). Mitochondrial genetics: A paradigm for aging and degenerative diseases? *Science, 256*, 628-632. doi: 10.1126/science.1533953

Wallace, D. C. (1999). Mitochondrial diseases in man and mouse. *Science*, *283*, 1482-1488. doi: 10.1126/science.283.5407.1482

Winklhofer, K. F., & Haass, C. (2011). Mitochondrial dysfunction in Parkinson's disease. *Biochimica Et Biophysica Acta (BBA) - Molecular Basis of Disease*, *1802*, 29-44. doi: 10.4061/2011/716871

Xu, K., Xu, Y. H., Chen, J. F., & Schwarzschild, M. A. (2002). Caffeine's neuroprotection against 1-methyl-4-phenyl-1, 2, 3, 6-tetrahydropyridine toxicity shows no tolerance to chronic caffeine administration in mice. *Neuroscience Letters*, *322*, 13-16. doi: 10.1016/S0304-3940(02)00069-1

Xu, K., Xu, Y. H., Chen, J. F., & Schwarzschild, M. A. (2010). Neuroprotection by caffeine: Time course and role of its metabolites in the MPTP model of Parkinson's disease. *Neuroscience, 167*, 475-481. doi: 10.1016/j.neuroscience.2010.02.020

Youle, R. J., & Strasser, A. (2008). The bcl-2 protein family: Opposing activities that mediate cell death. *Nature Reviews Molecular Cell Biology*, *9*, 47-59. doi: 10.1038/nrm2308

Zon, L. I., & Peterson, R. T. (2005). In vivo drug discovery in the zebrafish. *Nature Reviews Drug Discovery*, *4*, 35-44. doi: 10.1038/nrd1606

Appendix A: Confocal Trigger for Dark Flash Calcium Imaging

```
light = 1
confocal = 0

while (1)
if (confocal == 1)
     light = 0
     delay (var.delay)
     light = 1
     endif
endwhile
```

Appendix B: Spontaneous and Dimming Startle Script

```
while (1)
     while (var.capture == 1)
     //pixelink1 = 5
     pixelink1 = 5
     delay (.2)
     //pixelink1 = 0
     Pixelink1 = 0
     var.pics = var.pics +1
     delay (.79) // .5Hz frame rate
     endwhile
endwhile

//equal recording time before and after stim
var.capture = 0
var.taps = 0
var.trials = 0

delay (120)

while (var.numdims > var.dims)

//DIM
var.trials = var.trials +1
     toplight = 1
     var.capture = 1
     delay (car.prestim*60)
     lightled = 1
     highspeed = 1
     toplight = 0
     delay (var.lightoff*60)
     var.capture = 0
     highspeed = 0
     lightled = 0

     var.dims = var.dims +1 //count up another trial

end while

endseq(cameras)
toplight = 1
```

Appendix C: Spectral Analysis Script for Analyzing Calcium Oscillations

```
Treatment ={'PX'};%%These first two lines are for uploading
data from folders, probably not necessary

date={'6-21'};%%

close all

bin1 = [ .001 .01 .05 .1 1];%%setting the lower bounds for
the bins

bin2 = [ .01 .05 .1 1 2.5];%%setting the upper bounds for
the bins

color=('bgrk');%%colors for graphing different data sets

Exp_cond = ([Control, low_dose, med_dose,
high_dose]);%%list of data sets to be analyzed

for j=1%:4

x = Exp_cond(:,j);

dt=.2;

T=1200;


xf = fft(x);

Sxx = 2*dt^2/T * xf.*conj(xf); %2. Compute the power
spectrum.

Sxx = Sxx(1:length(x)/2+1); %3. Ignore negative
frequencies.

df = 1/max(T); %4. Determine the frequency resolution.

fNQ = 1/dt/2; %5. Calculate the Nyquist Frequency

faxis = (0:df:fNQ); %6. Construct the frequency axis.


C=sort(abs(Sxx),'descend'); % Finding dominant frequencies
```

```
norm=C(2); % Choosing largest frequency to normalize data


for i=1:length(bin1)

     J=intersect(find(faxis>=bin1(i)),find(faxis<=bin2(i)))
     ;%Determining indices in faxis corresponding to
     frequencies in bin i

     a=min(J);% index (in faxis) of lowest frequency in bin
     i

     b=max(J);%index (in faxis) of highest frequency in bin
     i

     A(a:b)=Sxx(a:b);%determining power of frequencies in
     bin i


     B = (Sxx(a:b)/norm); %normalizing bin i

     mean1(j,i+1)=real(mean(B));%calculating mean of bin i

     std1(j,i+1)=real(std(B));%calculating std of bin i

     clear A

     clear B

     clear J


end  % end for i

end % end for j


%%graph

errorbar(mean1(1,:),std1(1,:),color(1),'LineStyle','none')

hold on

plot((2:1:length(bin1)+1), mean1(1,2:6),[color(1)
'*'],'MarkerFaceColor',color(1))
```

```
errorbar(mean1(2,:),std1(2,:),color(2),'LineStyle','none')

plot((2:1:length(bin1)+1), mean1(2,2:6),[color(2)
'*'],'MarkerFaceColor',color(2))

errorbar(mean1(3,:),std1(3,:),color(3),'LineStyle','none')

plot((2:1:length(bin1)+1), mean1(3,2:6),[color(3)
'*'],'MarkerFaceColor',color(3))

errorbar(mean1(4,:),std1(4,:),color(4),'LineStyle','none')

plot((2:1:length(bin1)+1), mean1(4,2:6),[color(4)
'*'],'MarkerFaceColor',color(4))

xtick=[1 2 3 4 5 6 7 8];

myxticklabel={'','(0.001-0.01)','(0.01-0.05)','(0.05-
0.1)','(.1-1)','(1-2.5)','', ''}

set(gca,'XTick',xtick,'XTickLabels',myxticklabel,'Fontsize'
,12)

xlabel('Frequency ranges (Hz)','FontSize',14)

ylabel('Normalized power', 'FontSize',14)

legend('','Control','','40um','','100um','','200um')

title(['Normalized power of different frequencies, '
date{1} ' (' treatment{1} ')'],'FontSize',14)
```